Long Live Vinylidene! A New View of the $H_2C=C:$ → $HC \equiv CH$ Rearrangement from ab Initio Molecular Dynamics

Robin L. Hayes, Eyal Fattal, Niranjan Govind, and Emily A. Carter*

Contribution from the Department of Chemistry and Biochemistry, Box 951569, University of California, Los Angeles, California 90095-1569

Abstract: We present complete active space self-consistent field (CASSCF) ab initio molecular dynamics (AIMD) simulations of the preparation of the metastable species vinylidene, and its subsequent, highly exothermic isomerization to acetylene, via electron removal from vinylidene anion ($D_2C=C^- \rightarrow D_2C=C:$ → $DC \equiv CD$). After equilibrating vinylidene anion-d_2 at either 600 ± 300 K (slightly below the isomerization barrier) or 1440 K ± 720 K (just above the isomerization barrier), we remove an electron to form a vibrationally excited singlet vinylidene-d_2 and follow its dynamical evolution for 1.0 ps. Remarkably, we find that *none* of the vinylidenes equilibrated at 600 K and *only* 20% of the vinylidenes equilibrated at 1440 K isomerized, suggesting average lifetimes >1 ps for vibrationally excited vinylidene-d_2. Since the anion and neutral vinylidene are structurally similar, and yet extremely different geometrically from the isomerization transition state (TS), neutral vinylidene is *not* formed near the TS so that it must live until it has sufficient instantaneous kinetic energy in the correct vibrational mode(s). The origin of the delay is explained via both orbital rearrangement and intramolecular vibrational energy redistribution (IVR) effects. Unique signatures of the isomerization dynamics are revealed in the anharmonic vibrational frequencies extracted from the AIMD, which should be observable by ultrafast vibrational spectroscopy and in fact are consistent with currently available experimental spectra. Most interestingly, of those trajectories that did isomerize, every one of them violated conventional transition-state theory by recrossing back to vinylidene multiple times, against conventional notions that expect highly exothermic reactions to be irreversible. The dynamical motion responsible for the multiple barrier recrossings involves strong mode-coupling between the vinylidene CD_2 rock and a local acetylene DCC bend mode that has been recently observed experimentally. The multiple barrier recrossings can be used, via a generalized definition of lifetime, to reconcile extremely disparate experimental estimates of vinylidene's lifetime (differing by at least 6 orders of magnitude). Last, a caveat: These results are constrained by the approximations inherent in the simulation (classical nuclear motion, neglect of rotation−vibration coupling, and restriction to C_s symmetry); refinement of these predictions may be necessary when more exact simulations someday become feasible.

I. Introduction

Isomerization reactions that involve migrating hydrogen atoms, such as 1,2-hydrogen shifts, keto/enol tautomerization, and carbocation rearrangements, often play a critical role in more complex chemical reactions, such as dehydration of alcohols or hydration of alkenes.[1] These types of rearrangements are also involved in the gas-phase combustion of hydrocarbons.[2] Furthermore, such 1,2-hydrogen-shifts are central to the decomposition of carbenes[3,4] and nitrenes.[5] A precise spectroscopic

characterization of the dynamics would yield deeper insight into the mechanisms of such reactions. However, the ultrafast time scales, small barriers to rearrangement, breaking/forming of bonds, and the time-intensive nature of theoretical calculations make these processes challenging to investigate. An experimental strategy for investigating such metastable intermediates has been to prepare negative ions in the gas-phase whose structure, upon removal of an electron, may be close to the neutral transition state (TS) of the chemical reaction of interest.[6] In the current work, we have chosen to investigate theoretically the dynamics of one of the simplest isomerization reactions involving hydrogen: the rearrangement of vinylidene ($D_2C=C:$) to acetylene ($DC \equiv CD$), for which the relevant negative ion photodetachment experiments have already been performed.[7,8]

While vinylidene has been conjectured as an intermediate in both organic reactions[9] and in heterogeneous catalysis,[10] the very existence of vinylidene remained questionable for some time because of the small barrier to isomerization to produce the much more stable acetylene isomer. Negative ion photoelectron

(1) Solomons, T. W. G. *Organic Chemistry*, 6th ed.; John Wiley & Sons: New York, 1996.

(2) Dibble, R. W.; Warnatz, J.; Maas, U. *Combustion: Physical and Chemical Fundamentals, Modeling and Simulation, Experiments, Pollutant Formation,* 2nd ed.; Springer-Verlag: New York, 1999.

(3) (a) Skell, P. S.; Fagone, F. A.; Klabunde, K. J. *J. Am. Chem. Soc.* **1972**, *94*, 7862. (b) Reiser, C.; Steinfeld, J. I. *J. Phys. Chem.* **1979**, *84*, 680. (c) Reiser, C.; Lussier, F. M.; Jensen, C. C.; Steinfeld, J. I. *J. Am. Chem. Soc.* **1979**, *101*, 350.

(4) (a) Evanseck, J. D.; Houk, K. N. *J. Phys. Chem.* **1990**, *94*, 5518. (b) *J. Am. Chem. Soc.* **1990**, *112*, 9148. (c) Ma, B.; Schaefer, H. F., III. *J. Am. Chem. Soc.* **1994**, *116*, 3539.

(5) (a) Travers, M. J.; Cowles, D. C.; Clifford, E. P.; Ellison, G. B. *J. Am. Chem. Soc.* **1992**, *114*, 8699. (b) Travers, M. J.; Cowles, D. C.; Clifford, E. P.; Ellison, G. B.; Engelking, P. C. *J. Chem. Phys.* **1999**, *111*, 5349. (c) Richards, C.; Meredith, C.; Kim, S. J.; Quelch, G. E.; Schaefer, H. F., III. **1994**, *100*, 481.

(6) Neumark, D. M. *Acc. Chem. Res.* **1993**, *26*, 33.

(7) Burnett, S. M.; Stevens, A. E.; Feigerle, C. S.; Lineberger, W. C. *Chem. Phys. Lett.* **1983**, *100*, 124.

(8) Ervin, K. M.; Ho, J.; Lineberger, W. C. *J. Chem. Phys.* **1989**, *91*, 5974.

detachment proved useful for isolating metastable vinylidene in the gas phase. Burnett et al.[7] initially observed the highly unstable singlet vinylidene in 1983 by photodetaching an electron from the stable vinylidene anion ($H_2C=C^-$).[11] Several years later, Ervin, Ho, and Lineberger[8] refined the photoelectron detachment experiment to obtain more precise results. Another strategy has been to use stimulated emission pumping (SEP) to study the dynamics of the reverse reaction, $HC\equiv CH \rightarrow H_2C=C:$. Field, Kinsey, and co-workers[12] used SEP of acetylene to observe resonances associated with acetylene isomerization to vinylidene. The likely existence of such resonances was confirmed recently via quantum reaction probability calculations by Germann and Miller.[13] A very recent series of dispersed fluorescence experiments and analysis by Jacobson et al. examined short time scale (~1 ps) bending dynamics of highly vibrationally excited acetylene up to near the threshold for the reverse reaction taking acetylene to vinylidene.[14,15] Direct comparisons of our predictions to both sets of experiments—originating either with vinylidene or with acetylene—are made below. The practical importance of the reverse reaction, $HC\equiv CH \rightarrow H_2CC:$, has been convincingly demonstrated in kinetic analyses of acetylene combustion, where omission of this isomerization leads to a large error in the deduced acetylene C−H bond energy. Only inclusion of the acetylene−vinylidene isomerization into the kinetic analyses brings the derived thermochemistry in line with independent measurements.[16]

Given the metastability of vinylidene, it is of primary interest to determine its lifetime. From the ultraviolet negative ion photoelectron spectrum (NIPES) for singlet vinylidene, Ervin et al.[8] estimated a lower bound to the vinylidene lifetime of 0.027 ps, extracted from the vibrational origin peak width, which was further extrapolated to 0.04 to 0.20 ps using a line shape analysis. Note that the NIPES experiments only probe at most the first few hundred fs associated with the time during which the photoelectron is ejected and hence the measurement cannot probe the dynamics at longer times—therefore the interpretation of the experiments is limited to providing a lower bound. Early semiclassical dynamics calculations of the isomerization rate using a reaction path Hamiltonian, on a reduced dimension potential energy surface (PES) derived from single and double configuration interaction (SDCI) calculations, predicted vinylidene lifetimes of 0.2−4.6 ps,[17] consistent with the lower bounds derived from the NIPES experiments. Recently, quantum

dynamics[18,19] on a reduced dimension PES constructed from coupled cluster (CCSD(T)) calculations predicted the survival probability of vinylidene. They observe that in the first 30 fs, vinylidene stays in its well, then up to ~200 fs[19] there is a rapid loss of some vinylidene population, followed by a significant long time tail that goes out further than the simulation time (10 ps).[18] The most recent of these quantum dynamics simulation suggest a lifetime for the ground-state vibrational state of vinylidene of 293 ps.[19] These results are also consistent with the NIPES data; however, artifacts in the quantum dynamics model, discussed in section III.H, call into question somewhat the reliability of those predictions.

The above experimental and theoretical work suggested that vinylidene lives only on a picosecond to subpicosecond time scale—a very short-lived intermediate indeed. Recently, Levin et al.[20] used coulomb explosion imaging techniques to examine the vinylidene−acetylene isomerization yet again. The experiment involves photodetachment of the vinylidene anion, followed by collision 3.5 μs later with a target, from which they are able to extract the nuclear positions of all the molecules at the moment of collision. They contend that 51% of the molecules they analyzed had the structure of vinylidene. From this finding, they instigated considerable renewed controversy by suggesting a dramatically longer vinylidene lifetime of at least 3.5 μs, which would have significant consequences for its reactivity and kinetics. This is clearly at odds with the NIPES measurements and interpretation, as well as with previous theory. A major contribution of the current work is to show how an understanding of the dynamics of the vinylidene, while undergoing isomerization, can in fact reconcile these two exceedingly disparate conclusions about vinylidene's lifetime.

Intimately connected with the lifetime of vinylidene is the activation barrier to isomerization (sometimes referred to as its well depth). The potential energy surface (PES) has been shown by quantum chemical calculations[16,18,21−23] to involve a very shallow well for $H_2C=C:$, a transition state (TS) with a half-linear structure where one H bridges the two C's, while the other H is roughly collinear with the two C's, and a very deep well for acetylene ($HC\equiv CH$). Figure 1 contains a schematic of the neutral vinylidene to acetylene reaction coordinate. Note that the entire isomerization reaction occurs in the molecular plane.

The energy difference between vinylidene and acetylene has been difficult to measure precisely because of the instability of vinylidene. Based upon the measured CH_2 rock frequency—which is closely connected to the isomerization reaction coordinate—and a thermochemical cycle, Ervin et al. estimated a lower bound for the vinylidene well depth of 1.3 kcal/mol (including zero point energy) and an isomerization exothermicity of 46.4 ± 5.5 kcal/mol,[8] later refined to 47.4 ± 4.0.[24] Currently, the best theoretical estimate of the exothermicity is 43.4 ± 0.6 kcal/mol, which lies just within the experimental error bars. This value was obtained by using the complete basis set (CBS) limit of CCSD(T) calculations, corrected via CCSDT calculations in

(9) (a) Skell, P. S.; Plonka, J. H. *J. Am. Chem. Soc.* **1970**, *92*, 5620. (b) Davison, P.; Frey, H. M.; Walsh, R. *Chem. Phys. Lett.* **1985**, *120*, 227. (c) Duran, R. P.; Amorebieta, V. T.; Colussi, A. J. *J. Am. Chem. Soc.* **1987**, *109*, 3154. (d) Kiefer, J. H.; Mitchell, K. I.; Kern, R. D.; Yong, J. N. *J. Phys. Chem.* **1988**, *92*, 677.

(10) (a) Carter, E. A.; Koel, B. E. *Surf. Sci.* **1990**, *226*, 339. (b) Ormerod, R. M.; Lambert, R. M.; Hoffmann, H.; Zaera, F., Wang, L. R.; Bennett, P. W.; Tysoe, W. T. *J. Phys. Chem.* **1994**, *98*, 2134.

(11) Jensen, M. J.; Pedersen, U. V.; Andersen, L. H. *Phys. Rev. Lett.* **2000**, *84*, 1128.

(12) (a) Chen, Y.; Jonas, D. M.; Hamilton, C. E.; Green, P. G.; Kinsey, J. L.; Field, R. W. *Ber. Bunsen-Ges. Phys. Chem.* **1988**, *92*, 329. (b) Chen, Y.; Jonas, D. M.; Kinsey, J. L.; Field, R. W. *J. Chem. Phys.* **1989**, *91*, 3976.

(13) Germann, T. C.; Miller, W. H. *J. Chem. Phys.* **1998**, *109*, 94.

(14) (a) O'Brien, J.P.; Jacobson, M. P.; Sokol, J. J.; Coy, S. L.; Field, R. W. *J. Chem. Phys.* **1998**, *108*, 7100. (b) Jacobson, M. P.; O'Brien, J. P.; Silbey, R. J.; Field, R. W. *J. Chem. Phys.* **1998**, *109*, 121. (c) Jacobson, M. P.; O'Brien, J. P.; Field, R. W. *J. Chem. Phys.* **1998**, *109*, 3831. (d) Jacobson, M. P.; Silbey, R. J.; Field, R. W. *J. Chem. Phys.* **1999**, *110*, 845. (e) Jacobson, M. P.; Jung, C.; Taylor, H. S.; Field, R. W. *J. Chem. Phys.* **1999**, *111*, 600.

(15) Jacobson, M. P.; Field, R. W. *J. Phys. Chem. A* **2000**, *104*, 3073.

(16) Kiefer, J. H.; Mudipalli, P. S.; Wagner, A. F.; Harding, L. *J. Chem. Phys.* **1996**, *105*, 8075.

(17) Carrington Jr., T.; Hubbard, L. M.; Schaefer, H. F., III; Miller, W. H. *J. Chem. Phys.* **1984**, *80*, 4347.

(18) Schork, R.; Köppel, H. *Theor. Chem. Acc.* **1998**, *100*, 204.

(19) Schork, R.; Köppel, H. *Chem. Phys. Lett.* **2000**, *326*, 277.

(20) Levin, J.; Feldman, H.; Baer, A.; Ben-Hamu, D.; Herber, O.; Zaifman, D.; Vager, Z. *Phys. Rev. Lett.* **1998**, *81*, 3347.

(21) Gallo, M. M.; Hamilton, T. P.; Schaefer, H. F., III. *J. Am. Chem. Soc.* **1990**, *112*, 8714.

(22) Smith, B. J.; Smernik, R.; Radom, L. *Chem. Phys. Lett.* **1992**, *188*, 589.

(23) Chang, N.-Y.; Shen, M.-Y.; Yu, C.-H. *J. Chem. Phys.* **1997**, *106*, 3237.

(24) Ervin, K. M.; Gronert, S.; Barlow, S. E.; Gilles, M. K.; Harrison, A. G.; Bierbaum, V. M.; DePuy, C. H.; Lineberger, W. C.; Ellison, G. B. *J. Am. Chem. Soc.* **1990**, *112*, 5750.
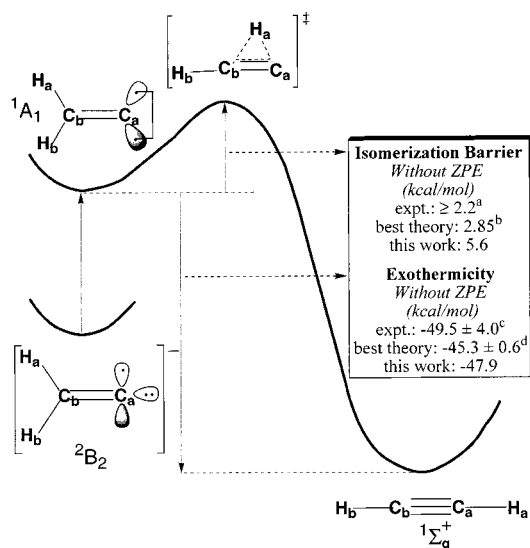
Figure 1. Schematic of the electron-detachment-induced isomerization of vinylidene to acetylene via the vinylidene radical anion. Energetics shown represent the best values available for the barrier height and exothermicity from experiment and theory, as well as those calculated here for the dynamics. They are shown without ZPE corrections since the AIMD simulations are carried out on the classical Born–Oppenheimer surface. References (a)–(d) shown here refer to the following footnotes in Table 3: *f*, *e*, *m*, and *k*, respectively. These explain how these values were derived. *CASSCF(10/10) describes the exothermicity well, while the barrier is likely too high by 2.8 kcal/mol.*

a finite basis*,* zero point energies, relativistic effects, and corrections for Born–Oppenheimer breakdown.[25,26]

The barrier to isomerization has been calculated including various levels of dynamic electron correlation and basis set, with the classical barrier (without zero point energy) falling between 2 and 3 kcal/mol.[18,21,23,27] The most accurate determination, involving CCSD(TQ) and extrapolations to both the CBS and full correlation limits,[23] places the isomerization transition state at 2.85 kcal/mol above the bottom of the vinylidene well. Using the best available theoretical estimates of zero point energy (ZPE) corrections,[23] one can remove the ZPE from the experimental lower bound for the barrier (≥ 1.3 kcal/mol) to obtain an "experimental" lower bound for the classical barrier height. This latter value turns out to be ≥ 2.2 kcal/mol, which is consistent with the best theoretical estimate of 2.85 kcal/mol.

In the work presented here, we will see that our method of calculation yields barrier heights and exothermicities consistent with experimental values, though slightly off from the best theoretical estimates. However, our primary focus is to go beyond energetics, to learn about dynamical behavior (e.g., anharmonic vibrations, isomerization dynamics, and the lifetime of vinylidene). For this, one must carry out time-dependent simulations of atomic motion.

The theoretical techniques for modeling the dynamics of ultrafast molecular processes are distinguished first by how the forces on the nuclei are calculated and second, by whether classical or quantal motion of the nuclei is considered. The most accurate, and in general the most time-consuming, technique for calculating the forces is to construct the entire PES (including all relevant degrees of freedom) using a method that accounts

for a high level of electron correlation. Generally, this is done in reduced dimensional spaces, or else the number of points at which the PES must be calculated becomes prohibitive. This can reduce the accuracy of the representation of the PES and can limit the predictive power of the dynamics.

An alternative strategy generates a PES on which to carry out dynamics in the full dimensional space by fitting a many-body analytic potential function. The problem with such an approach is that the choice of function constrains the dynamics observed, and it is generally not obvious what functional form would be appropriate for a case where multiple bonds are being broken and formed. Moreover, from a practical point of view, the fitting is a tedious and not always successful process. Either of these two strategies for PES construction can then be followed by running classical trajectories[28] or quantum wave packet dynamics.[29]

Currently available vinylidene−acetylene PES's[18,30,31] have some serious deficiencies. Artifacts among the pre-1990 PES's[30,31] include reaction barriers approximately a factor of 3 too large (up to 6 kcal/mol too high), as well as unphysical features such as allowed overlaps of C and H atoms.[13] A new PES derived from CCSD(T) calculations[18,19] represents a significant improvement in accuracy. However, it too suffers from unphysical limitations manifested subsequently in the quantum dynamics, which will be discussed later.

A third theoretical dynamics technique is ab initio molecular dynamics (AIMD).[32] In AIMD methods, the forces are derived from first principles quantum mechanics while the nuclei are propagated via classical mechanics subject to quantum-derived forces. AIMD allows one to explore dynamics on the full PES and the dynamics are not biased by a choice of analytic form for an interatomic potential function. The beauty of AIMD is the ability to generate qualitatively accurate and easily interpretable trajectories without the expense of constructing a global PES a priori. However, as it is expensive to calculate analytic gradients at every time step, drawbacks do exist with AIMD:

(i) the number (tens rather than thousands) and length (picoseconds rather than nanoseconds) of trajectories are limited, which means that statistical averages will be poor;

(ii) the level of ab initio theory that can be used in AIMD is not generally quantitatively accurate (errors of a few kcal/mol);

(iii) the systems studied are typically limited to classical dynamics on the ground-state PES, though extensions to nonadiabatic dynamics[33] and coupling to quantum dynamics[34,35] have been achieved recently.

Despite these limitations, one can use this technique to gain considerable qualitative insight via a representative set of trajectories. AIMD of simple molecular reactions have employed, for example, variants of Hartree−Fock theory [e.g., in the reactions of: $F + C_2H_4$,[36] thymine dimer with its cation,[37]

(25) Stanton, J. F.; Gauss, J. *J. Chem. Phys.* **1999**, *110*, 1831.

(26) For a thorough review of methods and basis set effects, see also: Peterson, K. A.; Dunning, T. H., Jr. *J. Chem. Phys.* **1997**, *106*, 4119.

(27) (a) Chen, W.-C.; Yu, C.-H. *Chem. Phys. Lett.* **1997**, *277*, 245. (b) Semprini, E.; Palma, A.; Stefani, F. *THEOCHEM* **1993**, *99*, 133. (c) Halvick, Ph.; Liotard, D.; Rayez, J. C. *Chem. Phys.* **1993**, *177*, 69.

(28) Tully, J. C.; Preston, R. K. *J. Chem. Phys.* **1971**, *55*, 562.

(29) Kosloff, R.; ed. Wyatt, R. E.; Zhang, J. Z. *Dynamics of Molecules and Chemical Reactions*; Marcel Dekker: New York, 1996; pp 185−230.

(30) (a) Carter, S.; Mills, I. M.; Murrell, J. N. *Mol. Phys.* **1980**, *41*, 191. (b) Halonen, L.; Child, M. S.; Carter, S. *Mol. Phys.* **1982**, *47*, 1097.

(31) Holme, T. A.; Levine, R. D. *Chem. Phys.* **1989**, *131*, 169.

(32) Car, R.; Parrinello, M. *Phys. Rev. Lett.* **1985**, *55*, 2471.

(33) (a) Ben-Nun, M.; Martinez, T. J. *J. Chem. Phys.* **1999**, *110*, 4134. (b) Thompson, K.; Martinez, T. J. *J. Chem. Phys.* **1999**, *110*, 1376. (c) Ben-Nun, M.; Martinez, T. J. *Chem. Phys. Lett.* **1998**, *298*, 57. (d) Martinez, T. J. *Chem. Phys. Lett.* **1997**, *272*, 139. (e) Martinez, T. J.; Levine, R. D. *J. Chem. Phys.* **1996**, *105*, 6334.

(34) (a) Miura, S.; Tuckerman, M.E.; Klein, M. L. *J. Chem. Phys.* **1998,** *109*, 5290. (b) Tuckerman, M. E.; Marx, D.; Klein, M. L.; Parrinello, M. *J. Chem. Phys.* **1996**, *104*, 5579. (c) Marx, D.; Parrinello, M. *J. Chem. Phys.* **1996**, *104*, 4077.

(35) Pavese, M.; Berard, D.R.; Voth, G. A. *Chem. Phys. Lett.* **1999**, *300*, 93.

CH$_2$O$^-$ with H$_3$CCl,[38] and H$_2$O + H$_3$CCl[39]], density functional theory (e.g., HO + NO$_2$[40] and a double proton transfer in (HCOOH)$_2$[41]) and complete-active-space self-consistent-field (CASSCF) theory [e.g., F + H$_2$ → FH + H[42]] for evaluation of the forces on the atoms.

The isomerization of vinylidene (H$_2$C=C:) to acetylene (HC≡CH) occurs on a potential energy surface that is highly anharmonic due to multiple bonds breaking and forming. Such a significant rearrangement of the electrons would be difficult to capture in an analytic potential energy function. Hence, AIMD is the ideal method for simulating and characterizing the dynamics of this system. Ideally, one would carry out a full-blown quantum dynamics simulation on a well-fit, accurate PES in the full rotation–vibration coordinate space (imposing no symmetry and propagating 9 degrees of freedom), but this is currently beyond reach computationally. Thus, AIMD represents a practical, albeit approximate, strategy for now. Even to carry out the AIMD simulations, it is necessary to make a minor compromise on accuracy, as we discuss below. However, we compensate for this small error (in the barrier height) in a logical manner (vide infra).

The goals of our study are to:

(i) elucidate the physical origin of the isomerization barrier,

(ii) gain further insight into dynamics at times beyond that probed by the NIPES experiment,

(iii) obtain a characteristic spectral signature of ultrafast isomerization dynamics,

(iv) explore the applicability of transition-state theory (TST), and

(v) explain the seemingly incompatible experimental lifetimes in the context of vibrational modes (both normal and local) and intramolecular vibrational energy redistribution (IVR).

In this work, we simulate with AIMD and create a picture of the dynamics to isolate the molecular motion and characteristic time scales for isomerization (related to the metastable reactants' lifetime) and compare our results to previous experimental and theoretical studies. Then, we calculate vibrational spectra to compare with the vibrational fine structure seen in the NIPES experiments. We will see, e.g., that the AIMD simulations reveal a dynamics in which the factors promoting isomerization, the vinylidene lifetime, and the validity of TST are closely tied to the extent of vibrational mode coupling between vinylidene and acetylene. Section II describes the calculations in more detail. Section III contains the results and discussion, and concluding remarks are included in Section IV.

II. Calculational Details

A. Basis Sets. The molecules were described by the 6-31G**[2+] Gaussian basis sets of Frisch, Pople, and Binkley,[43] which are valence double-ζ basis sets with one set of diffuse and one set of polarization functions on each atom. Although Chang et al.[23] showed that a simple double-ζ basis set raises the reaction barrier by 1.5−2.7 kcal/mol and

lowers the exothermicity by 4 kcal/mol compared to a triple-ζ basis, the size of the triple-ζ basis would make the AIMD prohibitively expensive. Consequently, the use of one set each of diffuse and polarization functions is an acceptable compromise between accuracy and speed.

B. Structural Optimization. GVB(5/10)-PP. Initially, the wave functions and structures of vinylidene, vinylidene anion, and acetylene were optimized at the generalized valence bond with perfect pairing (GVB-PP)[44] level using the PSGVB code.[45] In each case, five electron pairs were described with 10 natural orbitals. Vinylidene and the vinylidene anion employed the following correlated GVB pairs: 2 C−H bonds, 1 C−C σ bond, 1 C−C π bond, and 1 C lone pair. Acetylene utilized 2 C−H bonds, 1 C−C σ bond, and 2 C−C π bonds within GVB pairs. The C$_{1s}$'s were treated at the closed shell Hartree−Fock level. The orbitals of the GVB-PP wave functions were then used as input to the CASSCF calculations.

CASSCF (10 electrons/10 orbitals). Full valence CASSCF calculations were performed in HONDO.[46] All valence electrons were correlated, where the active space included all the natural orbitals from the GVB-PP(5/10) calculation, resulting in a 10 electron/10 orbital CASSCF calculation. C$_s$ symmetry was imposed for all the molecules. Both the vinylidene and the acetylene CASSCF expansions consisted of 19 404 spin eigenfunctions, while the vinylidene anion CASSCF expansion was comprised of 53 136 spin eigenfunctions. To decrease the amount of time per cycle for H$_2$C=C$^-$, we chose a slightly restricted active space in which the (out-of-plane) π bond, which is orthogonal to the reaction coordinate, was described only at the GVB-PP level. The resulting GVB(π_x/π_x^*)* CASSCF (9/9) calculation reduced the number of spin eigenfunctions to 53 004, at the negligible energy cost of 1×10^{-6} hartrees.

Search for the Transition State. The DIIS-Ridge method,[47] with a convergence criterion of 1×10^{-3} hartrees/bohr for the gradient at the CASSCF level of theory, was used to find the transition state. Normal-mode frequencies were calculated via diagonalization of the Hessian (energy second derivative) matrix, which was constructed via finite difference of analytic energy gradients at the CASSCF level. Identification of a single imaginary normal mode calculated from diagonalization of the Hessian matrix confirmed the rank of the saddle point (1) and identified it as a true transition state.

C. Ab Initio Molecular Dynamics and Analysis. Several methods exist for calculating forces on the atoms from quantum mechanics and propagating the nuclei classically. Generally, one either carries out an extended Lagrangian (fictitious wave function) dynamics as first proposed by Car and Parrinello[32] or one optimizes the wave function at each time step, staying on the Born−Oppenheimer surface.[42,48] Both Parrinello[49] and Gibson et al.[50] provide an in-depth discussion of the merits of both approaches. Here, we choose Born−Oppenheimer ab initio molecular dynamics (BO-AIMD), where the wave function is fully converged to the BO surface at each time step. Both the energies and the ab initio forces were calculated using the aforementioned CASSCF method. Newton's equations of motion for the nuclei were numerically integrated using the velocity-Verlet algorithm.[51] To make

(36) Bolton, K.; Hase, W. L.; Schlegel, H. B.; Kihyung Song. *Chem. Phys. Lett.* **1998**, *288*, 621.

(37) Aida, M.; Kaneko, M.; Dupuis, M.; Ueda, T.; Ushizawa, K.; Ito, G.; Kumakura, A.; Tsuboi, M. *Spectrochim. Acta* **1997**, *53A*, 393.

(38) Yamataka, H.; Aida, M.; Dupuis, M. *Chem. Phys. Lett.* **1999**, *300*, 583.

(39) Aida, M.; Yamataka, H.; Dupuis, M., *Chem. Phys. Lett.* **1998**, *292*, 474.

(40) Doclo, K.; Rothlisberger, U. *Chem. Phys. Lett.* **1998**, *297*, 205.

(41) Miura, S.; Tuckerman, M.E.; Klein, M. L. *J. Chem. Phys.* **1998**, *109*, 5290.

(42) da Silva, A. J. R.; Cheng, H.-Y.; Gibson, D. A.; Sorge, K. L.; Liu, Z.; Carter, E. A. *Spectrochim. Acta.* **1997**, *53*, 1285.

(43) Frisch, M. J.; Pople, J. A.; Binkley, J. S. *J. Chem. Phys.* **1984**, *80*, 3265.

(44) Bobrowicz, F. W.; Goddard, W. A., III. *Methods of Electronic Structure Theory*; Plenum: New York, 1977; p 79.

(45) Ringnalda, M. N.; Langlois, J.-M.; Murphy, R. B.; Greeley, B. H.; Cortis, C.; Russo, T. V.; Marten, B.; Donnelly, R. E., Jr.; Pollard, W. T.; Cao, Y.; Muller, R. P.; Mainz, D. T.; Wright, J. R.; Miller, G. H.; Goddard, W. A., III; Friesner, R. A. *PS-GVB v2−3*; Schrodinger, Inc., 1996.

(46) Dupuis, M.; Johnston; F., Marquez, A. *HONDO 8.5 from CHEM-Station*; IBM Corporation: Kingston, NY, 1994.

(47) (a) Ionova, I. V.; Carter, E. A. *J. Chem. Phys*. **1995**, *103*, 5437. (b) Ionova, I. V.; Carter, E. A. *J. Chem. Phys*. **1993**, *98*, 6377.

(48) (a) Liu, Z.; Carter, L. E.; Carter, E. A. *J. Phys. Chem*. **1995**, *99*, 4355. (b) Chelikowsky, J. R.; Troullier, N.; Binggeli, N. *Phys. Rev. B* **1994,** *49*, 114. (c) Arias, T. A.; Payne, M. C.; Joannopoulos, J. D. *Phys. Rev. B* **1992**, *45*, 1538. (d) Barnett, R. N.; Landman, U.; Nitzan, A.; Rajagopal, G. *J. Chem. Phys*. **1991**, *94*, 608. (e) Wentzcovitch, R. M.; Martins, J. L. *Solid State Commun*. **1991**, 78, 831.

(49) Parrinello, M. *Solid State Commun*. **1997**, *102*, 107.

(50) Gibson, D. A.; Ionova, I. V.; Carter, E. A. *Chem. Phys. Lett*. **1995**, *240*, 261.

(51) Swope, W. C.; Andersen, H. C.; Berens, P. H.; Wilson, K. R. *J. Chem. Phys*. **1982**, *76*, 637.

Table 1. Bond Lengths (Å) and Bond Angles (deg) of C_2H_2 Isomers from CASSCF and CCSD(T) Calculations and from Experiment

structure[a]	$r(C_aC_b)$	$r(C_bH_a)$	$r(C_bH_b)$	$\theta(C_aC_bH_a)$	$\theta(C_aC_bH_b)$	ref
		$H_2C_2^-$				
CASSCF/6-31G**++	1.360	1.126		124.1		b
experiment	1.347±0.007	1.119±0.006		124.0±0.2		c
		Vinylidene (H₂CC:)				
CASSCF/6-31G**++	1.328	1.101		120.2		d
CCSD(T)/cc-pVTZ	1.300	1.081		120.03		23
""	1.3070	1.0862		120.08		26
CCSD(T)/cc-pVQZ	1.2993	1.0845		120.03±0.1		26
(+corrections)	±0.0005	±0.001				
		TS				
CASSCF/6-31G**++	1.278	1.345	1.087	56.4	177.2	d
CCSD(T)/cc-pVTZ	1.255	1.378	1.067	53.79	178.33	23
		Acetylene (HCCH)				
CASSCF/6-31G**++	1.225	1.077				d
CCSD(T)/cc-pVTZ	1.205	1.058				23
""	1.2097	1.0637				26
CCSD(T) /cc-pVQZ	1.2064	1.0633				26
experiment	1.2033	1.0605				56

[a] See Figure 1 for atom labeling. *[b]* This work; CASSCF(9/9) with two GVB-PP(π/π^*) reference states. *[c]* See ref 8. Estimated from geometry displacements obtained from a Franck−Condon simulation of Ervin et al.'s photoelectron spectra (ref 8) relative to the singlet state structure predicted from CI/TZ + P calculations by Carrington et al. (ref 17). *[d]* This work; CASSCF(10/10). See section II for details.

the CASSCF-MD calculations possible, we exploited the C_s symmetry present in all stationary points (minima and the transition state) in our trajectories. This is an added constraint, since out of plane distortions are neglected.

Vibrational Spectra. The filter diagonalization (FD) method[52,53] was used to determine anharmonic vibrational frequencies from velocity autocorrelation functions constructed from the AIMD trajectories.[54] FD has been shown already to be useful in extracting anharmonic frequencies from AIMD simulations.[55] Note this technique yields frequencies, but not intensities.

Dominant Normal-Mode Analysis. To qualitatively classify which normal mode of vibration is "most" active [$M_D(t)$] at a given time (t) during a trajectory, values for each vinylidene normal mode, $M_i(t)$, are defined via a scalar product, such that:

$$M_i(t) = \sum_j \dot{r}_j(t) \cdot \nu_{i,j} \quad M_D(t) = \text{Max}\{M_i(t)\}$$

where j ranges over all 4 atoms, $\dot{r}_j(t)$ is the velocity of atom j at time t, and $\nu_{i,j}$ is the normal mode displacement vector for atom j calculated at the CASSCF level corresponding to normal mode ν_i. Qualitatively, the vinylidene normal mode that has the most overlap with the velocity components of the vinylidene will be the dominant normal mode, M_D. Note that this analysis by necessity neglects anharmonic vibrational corrections and does not distinguish between cases where two or more modes are equally dominant.

III. Results and Discussion

A. Optimized Structures. Table 1 compares the CASSCF-(10/10) bond lengths and angles for all four species to other published values.[8,17,23,26,56] Although our CASSCF(10/10) calculation slightly, yet consistently, overestimates the bond lengths by 1−2%, the bond angles are generally in excellent agreement with published values. A very slight discrepancy is found for

the H−C−C bond angle in the transition state [$\theta(C_aC_bH_a)$], which is larger by ≈3° relative to the angle predicted by the CCSD(T) /cc-pVTZ[23] level of theory.

More generally, though, our CASSCF transition state agrees closely with the predicted structure at the CCSD(T)/cc-pVTZ level. The ∼2% smaller bond length between the bridging hydrogen and the connecting carbon [$r(C_bH_a)$] results in our structure being slightly more similar to the vinylidene structure than the predicted geometry at the higher level of theory. However, the transition state is closer in geometry overall to acetylene than vinylidene. Clearly, the H−C−C bond angle [θ-($C_aC_bH_a$)] demonstrates that the transition state and the vinylidene anion possess significantly different geometries. This suggests that unless the barrier is sufficiently small, photodetachment of H_2CC^- may not yield a vinylidene structure close to the TS, hence isomerization may be inhibited. By contrast, the vinylidene and vinylidene anion are structurally very similar, as expected based upon previous studies.[57] The bonds are longer only by ∼2% and the H−C−C bond angle is only larger by 4° in the anion. Both trends are consistent with the addition of an extra nonbonding π-electron in the molecular plane (see Figure 1).

B. Harmonic Frequencies. Harmonic normal-mode frequencies are listed in Table 2. Since the normal mode calculations were computed without symmetry, CASSCF frequencies are calculated for all species except the vinylidene anion, where the large number of spin eigenfunctions prevented the calculation. As can be seen from the Table, our calculated harmonic normal modes for vinylidene, the transition state, and acetylene agree well with experimental and CCSD(T)−derived results. In general, the frequencies are within 3% of other published values. Notable exceptions include the CH₂ rock of vinylidene (ν_6), and the imaginary mode (ν_6) and the CH stretch (ν_1) of the transition state. However, the ν_6 mode corresponds to the reaction coordinate and is therefore expected—and indeed has been demonstrated[58]—to be quite anharmonic. Harmonic fre-

(52) Wall, M. R.; Neuhauser, D. *J. Chem. Phys.* **1995**, *102*, 8011.

(53) Mandelshtam, V. A.; Taylor, H. S. *Phys. Rev. Lett.* **1997**, *78*, 3274.

(54) A low-resolution fast Fourier transform (FFT) spectrum from our velocity autocorrelation signal was used as a guide. For the FD technique, overlapping energy bins of width 438.9 cm⁻¹ shifted by 219.5 cm⁻¹ were used to isolate the valid frequencies. A frequency was considered valid if it appeared within the inner 50% of all relevant energy bins with a large real weight and a small damping factor.

(55) da Silva, A. J. R.; Pang, J. W.; Carter, E. A.; Neuhauser, D. *J. Phys. Chem.* **1998**, *102*, 881.

(56) Strey, G.; Mills, I. M. *J. Mol. Spectrosc.* **1976**, *59*, 103.

(57) (a) Dawson, J. H.; Nibbering, N. M. M. *J. Am. Chem. Soc.* **1978**, *100*, 1928. (b) Dawson, J. H. J.; Jennings, K. R. *J. Chem. Soc., Faraday Trans.* **1976**, *272*, 700. (c) Lindinger, W.; Albritton, D. L.; Fehsenfeld, F. C.; Ferguson, E. E. *J. Chem. Phys.* **1975**, *63*, 3238. (d) Goode, G. C.; Jennings, K. R. *Adv. Mass. Spectrom.* **1974**, *6*, 797.

(58) Stanton, J. F.; Gauss, J. *J. Chem. Phys.* **1999**, *110*, 6079.

Table 2.   Harmonic Frequencies (cm^{-1}) of C_2H_2 and C_2D_2: CASSCF(10/10), CCSD(T) and Experiment

species	ν_1	ν_2	ν_3	ν_4	ν_5	ν_6
Vinylidene (H₂CC:)						
	CH sym str	CC str	CH₂ scissors	CH₂ wag	CH asym str	CH₂ rock
this work/ CASSCF	3045	1632	1242	775	3138	472
CCSD(T)/ TZ2P[a]	3144	1656	1238	743	3240	367
CCSD(T)/ cc-pVTZ[a]	3159	1682	1234	769	3228	327
CCSD(T)/cc-pCVTZ (anharmonic)[b]	2988	1653	1176	716	3065	263
CCSD(T)/cc-pVTZ (quantum dynamics)[c]		1671	1205			472(2ν)
experiment[d]	3025 ± 30	1635 ± 10	1165 ± 10			320[e]
						450 ± 30[f]
Transition State						
This work/ CASSCF	2417	1775	891	559	3275	807i
CCSD(T)/TZ2P[a]	2538	1799	897	560	3361	967i
CCSD(T)/cc-pVTZ[a]	2559	1821	905	575	3377	936i
Acetylene (HCCH)						
	CC str	CH asym str	CH sym str	HCCH cis-bend	HCCH trans-bend	
this work/ CASSCF	1975	3335	3425	750	622	
CCSD(T)/TZ2P[a]	2000	3393	3497	704	512	
CCSD(T)/cc-pVTZ[a]	2016	3409	3533	753	589	
experiment[g]	1974±3	3289±3	3374±6	730±1	612±6	
Vinylidene-d₂ (D₂CC:)						
	CD sym str	CC str	CD₂ scissors	CD₂ wag	CD asym	CD₂ rock
this work/ CASSCF	2234	1570	914	618	2330	372
CCSD/TZ+2P[h]	2318	1626	915	610	2417	305
experiment[d]	2190 ± 30	1590 ± 20	865 ± 10			250[e]
						370 ± 30[f]
Transition State - d₂						
this work/ CASSCF	1750	1675	695	444	2499	602i
Acetylene-d₂ (DCCD)						
	CC str	CD asym str	CD sym str	DCCD cis-bend	DCCD trans-bend	
this work/ CASSCF	1760	2449	2718	551	518	
experiment[g]	1762 ± 6	2439 ± 1	2701 ± 6	537 ± 1	505 ± 6	
D₂CC⁻						
	CD sym str	CC str	CD₂ scissors	CD₂ wag	CD asym str	CD₂ rock
expt, [HF/6-31+G**][i]	[2231]	[1503]	960 ± 20	[681]	[2281]	[787]

[a] Reference 23. [b] Standard vibrational anharmonicity using second order perturbation theory, ref 58. [c] Extracted from fine structure of calculated photoelectron spectrum, ref 19. [d] Reference 8. [e] Value based on CH₂ rock (ν_6) anion $\nu = 1$ to neutral $\nu = 1$ transition frequency (relative to the CH₂ rock (ν_6) anion $\nu = 0$ to neutral $\nu = 0$ transition frequency) and estimated anion CH₂ rock (ν_6) $\nu = 0$ to $\nu = 1$ transition frequency, ref 8. [f] Actual measurement; assignment uncertain, ref 8. [g] Reference 59. [h] Reference 21. [i] Those values in [] are from HF/6-31+G** calculations, ref 8.

quencies for the deuterated species are also shown for future comparison with our anharmonic frequencies derived via the filter diagonalization (FD) technique. Our CASSCF-derived harmonic frequencies for DC≡CD are within 3% of the experimental values.[59] Unfortunately, few published anharmonic frequencies of H₂C=C: and H₂C=C⁻ are available for comparison with our results, although Stanton and Gauss[58] have recently published anharmonic frequencies at the CCSD(T) level for H₂C=C: and H₂C=C⁻ and Schork and Köppel[18,19] extracted anharmonic frequencies via quantum wave packet dynamics for H₂C=C:. These are also shown in Table 2. Our predicted frequencies for D₂C=C: are consistent with the experimental values.

C. Reaction Energetics. Figure 1 pictorially depicts the electron detachment from the anion to the neutral potential energy surface near the vinylidene equilibrium geometry, followed by the subsequent isomerization to acetylene across

(59) Shimanouchi, T. *Tables of Molecular Vibrational Frequencies Consolidated*; National Bureau of Standards: Washington, DC, 1972; Vol. 1, pp 1−160.

the small barrier. Table 3 compares our CASSCF(10/10) total energies for the optimized structures, along with our predicted isomerization barrier height and exothermicity, to values obtained at the CCSD(T) level. In our CASSCF calculation, the electron affinity (EA) of vinylidene is −7.1 kcal/mol compared to the experimental adiabatic EA of 11.3 ± 0.1 kcal/mol.[8] EA's are notoriously difficult to calculate accurately without extremely large basis sets. However, a larger basis set would preclude the AIMD simulation. The metastability of our anion with respect to neutral vinylidene is not particularly relevant, since the dynamics on the anion PES are merely used to prepare the initial state of neutral vinylidene. Since the anion does not autoionize in our simulations, we can use dynamics on this PES for such state preparation.

What is of primary importance for physically valid isomerization dynamics is the accuracy of the neutral PES, not the anion PES. At the CASSCF level, the barrier height is overestimated by 2.8 kcal/mol with respect to the Full CI (FCI)/complete basis set (CBS) calculation. The difference in barrier height will be important later when we consider the conditions

Table 3. Isomerization Barriers (E_a) and Exothermicities (ΔE) in kcal/mol with and without Zero-Point Corrections

species	CASSCF(10/10) total energy (hartrees)[a]	zero-point energies (ZPE; kcal/mol)		
		CASSCF (this work)[a]	CCSD(T)	expt
H₂CC:	−76.898374	14.7	14.87[b]	14.1[c]
D₂CC:		11.5		
[H₂CC]	−76.889400	12.7	13.21[b]	
[D2CC]		10.1		
HCCH	−76.974716	16.4	16.65[b], 16.46[d]	16.2[e]
DCCD		13.0		12.8

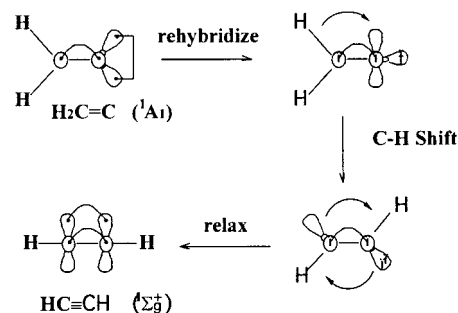| energies (kcal/mol)	CASSCF(10/10)	CCSD(T)	FCI/CBS[f]	expt
E_a	5.6[a]		2.85	≥2.2[g]
E_a w/ZPE	3.6[a]	1.1−1.5[h]		≥1.3[i]
E_a w/ZPE - d_2[j]	4.2[a]			
ΔE	−47.9[a], −49.1[k]	−45.3 ± 0.6[l]	−45.1	−49.5± 4.0[m]
ΔE w/ZPE	−46.2[a]	−42.95[b], −43.4± 0.6[n]		−47.4± 4.0[p]
ΔE w/ZPE - d_2[j]	-46.4[a]			

[a] This work; CASSCF(10/10) within a 6-31G**++ basis. See section II for details. [b] ZPE corrections calculated from the harmonic vibrational frequencies at the CCSD(T) level within a cc-pVTZ basis listed in ref 23. [c] Computed from the experimentally observed fundamental frequencies of ref 8 and the CCSD(T) anharmonic frequencies of ref 58. [d] Derived from experimental force fields. Values reported in refs 26 and 72. [e] Computed from the experimentally observed fundamental frequencies of ref 59. [f] Complete basis set extrapolation (See ref 23). [g] Minimum value based upon experimental estimate of E_a ≥ 1.3 kcal/mol, then corrected for ZPE via harmonic CCSD(T)/cc-pVTZ calculations for the TS (ZPE = 13.21 kcal/mol; ref 23) and experimental estimates for the vinylidene ZPE (14.1 kcal/mol; see footnote c). [h] Estimated in ref 23 from the FCI/CBS reaction barrier with ZPE corrections based on harmonic CCSD(T) calculations. Range due to corrections derived from experimentally observed frequencies. [i] See ref 8. [j] Includes ZPE on the deuterated species. [k] CASSCF(10/10) within an extended basis pV5Z/QZ (see ref 26). [l] Includes CCSDT, relativistic, and Born−Oppenheimer breakdown corrections (see ref 25). [m] Experimental value taken from ref 24 corrected with experimental estimates for the vinylidene ZPE (14.1 kcal/mol; see footnote c) and acetylene ZPE (16.2 kcal/mol; see footnote e). [n] Same as footnote k with ZPE taken from ref 25. [p] See ref 24.

for studying the isomerization dynamics. The CASSCF(10/10) exothermicity is approximately 6% larger than higher level calculations. However, by comparing the exothermicity of the CASSCF(10/10)/cc-pV5Z/QZ calculation to our value, the basis set effect is seen to be −1.2 kcal/mol. Thus, the missing dynamic correlation energy contribution to the exothermicity appears to be ∼4 kcal/mol. Note, however, that our exothermicity is within experimental error and the barrier height is consistent with the experimentally estimated lower bound of 2.2 kcal/mol. Consequently, our model should provide physically reasonable results.

Using our CASSCF(10/10) harmonic frequencies for both the hydrogenated and deuterated molecules, we calculated ZPE-corrected isomerization exothermicities and barriers. Table 3 also compares our CASSCF(10/10) values to experimental and CCSD(T) results. Our ZPE-corrected exothermicity is in excellent agreement with experiment, and our ZPE-corrected barrier height is consistent again with the experimental lower bound of 1.3 kcal/mol. However, since CCSD(T) values find a barrier closer to 1.5 kcal/mol, we appear to overestimate the ZPE-corrected barrier height by ∼2 kcal/mol.

Origin of Isomerization Barrier. Vinylidene has an unsaturated carbenoid carbon, whose lone pair of electrons is described well within a generalized valence bond (GVB) picture, as a singlet-coupled pair of singly occupied, overlapping sp²-hybrid-like orbitals (see Figure 1 and below) in the traditional GVB view of a singlet carbene.[60] In order for the 1,2-hydrogen shift to occur in a concerted fashion where electron *pairs* move during the rearrangement, one must think of the moving H atom as either a hydride, H⁻, or think of the entire C−H bond pair as moving. Either way, the low barrier to isomerization—predicted both by ab initio quantum chemistry and expected based on the Hammond postulate[61] due to the large reaction exothermicity—will require the presence of an empty orbital on the carbenoid carbon into which the moving pair of electrons may delocalize. The correlation of a low barrier with the presence of an empty orbital during isomerization was noted previously by Ervin et al.[8] This requires a rehybridization of the carbenoid lone pair

from sp² to sp, to free up the in-plane p-orbital to accept the incoming C−H electron pair, as shown below.

This rehybridization may be the quantum mechanical origin of the barrier in this reaction. We test this hypothesis below. Once the C−H bond pair has an empty p-orbital in which to donate, the rest of the process will be fast, as shown above. The 1,2-shift occurs, forming a transient charge-separated carbene intermediate, whose lone pair will be converted immediately to a C−C π bond of acetylene to remove the charge separation. *It may be that the role of the CH₂ rocking motion is to induce the sp² to sp lone pair rehybridization, to reduce nonbonded repulsions between the C−H bonds and the carbenoid lone pair.*

Similar analyses can be used to understand generally the rearrangements of other carbenes and nitrenes, such as methylcarbene to ethylene (H₃CH → H₂C=CH₂) and methylnitrene to methyleneimine (H₃CN → H₂C=NH).[5] Earlier calculations by Houk and co-workers[62] and Schaefer and co-workers[63] for the CH₃CH isomerization showed a similarly small barrier of 2−3 kcal/mol, consistent with this rehybridization mechanism as the origin of the barrier.
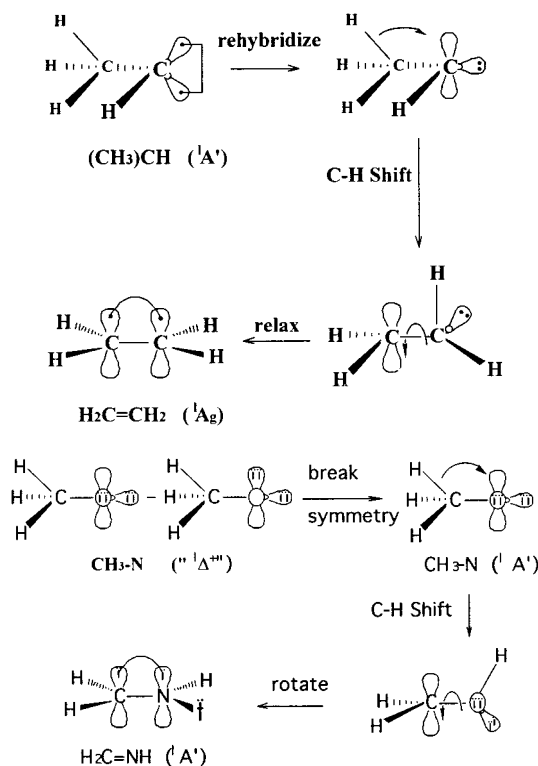
(60) Carter, E. A.; Goddard, W. A., III. *J. Chem. Phys.* **1988**, *88*, 1752.
(61) Hammond, G. S. *J. Am. Chem. Soc.* **1955**, *77*, 334.
(62) (a) Evanseck, J. D.; Houk, K. N. *J. Phys. Chem.* **1990**, *94*, 5518. (b) Evanseck, J. D.; Houk, K. N. *J. Am. Chem. Soc.* **1990**, *112*, 9148.
(63) Ma, B.; Schaefer, H. F. *J. Am. Chem. Soc.* **1994**, *116*, 3539.

(CH₃)CH (¹A′) rehybridize

C-H Shift

H₂C=CH₂ (¹Ag) relax

CH₃-N ("¹Δ⁺") break symmetry **CH₃-N (¹A′)**

C-H Shift

H₂C=NH (¹A′) rotate

We can estimate the cost of rehybridization of the carbenoid carbon in a simple calculation, by comparing the total energies for vinylidene calculated via Hartree−Fock (HF) theory and generalized valence bond (GVB) theory, where in the latter, only the carbenoid lone pair is correlated. The GVB calculation allows the C sp lone pair to sp²-hybridize by mixing in the empty in-plane C p-orbital, while in the HF calculation, the sp lone pair cannot do this. The difference between these two calculations may be taken as an estimate of the rehybridization cost. Using the CASSCF-optimized geometry for both the HF and GVB calculations, we find this difference to be 6.3 kcal/mol. This is strikingly similar to the 5.8 kcal/mol activation energy found at the CASSCF level. While not rigorous proof, it does provide compelling evidence that the origin of the barrier may indeed be the rehybridization energy cost.

D. Molecular Dynamics Trajectories. Initial Conditions. We emphasize again, this is a simulation where the nuclei are propagated according to classical dynamics on a Born−Oppenheimer PES, without accounting for quantum dynamical effects such as ZPE, tunneling, or rotation−vibration coupling. These approximations are described further below.

To properly model finite temperature dynamics on an approximate potential energy surface, the relative magnitude of the thermal energy k_bT and the barrier height should faithfully reproduce experiment. However, the "temperature" of a single molecule at a specific instant in time is an ill-defined quantity. Following the usual molecular dynamics convention, we characterize our simulation "temperature" as the kinetic temperature, which corresponds to the average kinetic energy of the molecule

$$\left[T_k = \frac{2\langle E_{\text{kin}} \rangle}{g k_B} \right]$$

In our case, there are 5 degrees of freedom, g, due to the removal of linear and angular momentum and the constraint of the molecule to be planar (vide infra). Very recently, Jellinek and

Goldberg[64] proposed that the correct vibrational "temperature" for microcanonical molecular dynamics simulations such as ours is

$$\left[T_m = \frac{2}{g' k_B \langle E_{kin}^{-1} \rangle} \right]$$

where $g' = g - 2$. Although both expressions lead to the same thermodynamic limit, T_m is consistently larger than T_k.

Since, as discussed earlier, our Born−Oppenheimer barrier height is overestimated by a factor of 2 (5.6 vs 2.8 kcal/mol), it is logical to scale the experimental temperature accordingly when choosing our simulation "temperature". This will make the modeled thermal energy consistent with our modeled barrier height. The exact experimental temperature has a large uncertainty. Estimates include 315 ± 20 K[8], 220 ± 30 K[8], 150 ± 50K[8], and 300 K[65] based upon both the He buffer gas temperature and the rotational temperature of the OH⁻ byproduct produced along with $H_2C=C^-$, the photoelectron spectrum of CH_2- under similar conditions, the rotational line shapes of triplet $H_2C=C$:, and other estimates, respectively.

To model the experimental temperature of 300 ± 150 K, we ran trajectories at two different simulation "temperatures" (T_k): 600 K $\pm$ 300 K or 3.0 kcal/mol average kinetic energy, which is meant to explore the region just below the barrier top (5.6 kcal/mol), and 1440 ± 720 K or 7.1 kcal/mol average kinetic energy, which is intended to probe the region slightly above the barrier top. This is akin to assuming a He buffer gas has equilibrated the anions at these temperatures for all degrees of freedom. The initial conditions then were (i) the CASSCF(10/10) equilibrium geometry for the anion at 0 K and (ii) velocities chosen randomly from a Boltzmann distribution at 600K or 1440 K.

The reaction coordinate only involves vibrational degrees of freedom, not rotational ones. Therefore, we ignore rotation−vibration coupling and chose vibrational energies characteristic of the He buffer gas temperature (appropriately scaled) as stated above. Since rotation is not involved in the isomerization, we started our anion trajectories without angular momentum (i.e., in the $J = 0$ state) for simplicity of analysis. Therefore the total angular and linear momentum were set to zero at the beginning of the anion trajectories. These quantities were conserved to within 0.07 h and 0.10 h for all trajectories at 600 and 1440 K, respectively. The extent to which inclusion of vibrational−rotational coupling, such as Coriolis coupling, would change the results will have to await the day that higher dimensional dynamics calculations including rotation are feasible.

Since the reaction coordinate for isomerization is planar, we constrained all of the atoms to a plane by removing the components of the velocities perpendicular to the molecular plane, allowing us to exploit C_s symmetry in the wave function calculation. Inclusion of out-of-plane motion might have a small, but unpredictable effect on the vinylidene lifetime and barrier traversal dynamics, due to the competing processes of additional paths over the barrier available at finite temperature, which might increase isomerization, versus distribution of energy into nonplanar modes that might inhibit isomerization.

Finally, to increase the time step so that longer trajectories could be followed and to minimize the effects of ZPE and tunneling, both hydrogen atoms were replaced with deuterium atoms in the AIMD simulations. Since the experiments were done on both the deuterated and the protonated forms, this does

(64) Jellinek, J.; Goldberg, A. *J. Chem. Phys.* **2000**, *113*, 2570.
(65) W. C. Lineberger, private communication.

not affect our ability to compare with experiment. The incorporation of tunneling would increase the barrier crossing rate; consequently, our simulation will provide an upper bound to the initial lifetime of vinylidene and a lower bound on the number of transition-state crossings (vide infra).

Equilibration of Vinylidene Anion-d_2. Two sets of randomly chosen initial velocities (each properly scaled to the desired temperature) were used to begin two thermal equilibration trajectories of the vinylidene anion at each temperature (600 and 1440 K), using a time step of ~1.2 fs (50 au). The velocities were only rescaled whenever the instantaneous kinetic temperature exceeded the bounds of 600 ± 300 K or 1440 ± 720 K (The uncertainty in T,

$$\sigma_T = \frac{T}{\sqrt{N}}$$

where N = the number of atoms). After each trajectory thermally equilibrated the vinylidene anion at either 600 or 1440 K, six different energy-conserving (free dynamics) anion trajectories, referred to as An_{1-3}^{600} and An_{1-3}^{1400}, were started at different times simply by terminating the temperature rescaling. We scanned the thermalization trajectories to choose starting points for the free dynamics anion trajectories with some CD_2 rock motion so as to increase our chances of observing isomerization. Free dynamics trajectories An_{1-2}^{600} were initiated at 218.9 fs and 274.5 fs along the first 600 K thermalization trajectory, An_3^{600} was started at 291.5 fs along the second 600 K thermalization trajectory, An_{1-2}^{1400} were begun at 152.5 and 203.3 fs along the first 1440 K thermalization trajectory, and An_3^{1400} originated at 221.4 fs along the second 1440 K thermalization trajectory. Figure 2(a) displays the initial geometries and velocities of the An_{1-3}^{1400} trajectories, since the trajectories equilibrated at 1440 K display the more interesting isomerization behavior. The initial configurations of An_{1-3}^{600} are qualitatively similar to those of An_{1-3}^{1400}, but with smaller magnitude velocities. Both experiments[8] and theory[8,13,17,66] have verified that the CH_2 rock mode is the dominant mode associated with the reaction coordinate. Notice how An_3^{1400} appears more likely to be reactive than either An_1^{1400} or An_2^{1440} by the orientation of its initial velocities, which more closely resemble a rocking of the CD_2 group.

Electron Detachment to Neutral Vinylidene. Forty neutral vinylidene trajectories at 600 and 1440 K (20 each) were initiated by simulating electron detachment of ($^2B_2$) $D_2C=C^-$ to ($^1A_1$) $D_2C=C$:. This was accomplished by removing, at different fixed times along the anion trajectory, the radical electron from the in-plane π orbital (b_2 symmetry) to form singlet vinylidene (see Figure 1), maintaining the anion's coordinates and velocities at the instant of electron removal (see Figure 2b for initial conditions of the 20 trajectories generated from An_{1-3}^{1400}). This is a "vertical" transition, since photodetachment happens essentially instantaneously, causing the nuclei to be effectively "frozen" during the event (i.e., the coordinates and velocities remain unchanged.) Electron detachments at five ~50 fs intervals were taken from each of the An_1^{600}, An_1^{1440}-(ED_{1-5}^1), and An_2^{1440} (ED_{1-5}^2) trajectories, while electron detachments at 10 ~50 fs intervals were taken from each of the An_3^{600} and An_3^{1440} (ED_{1-10}^3) trajectories. The resulting neutral vinylidene trajectories were followed for 1 ps. Recall that Ervin et al. placed a lower bound on the lifetime of $D_2C=C$: of 0.033 ps and estimated that the lifetime was in the subpicosecond
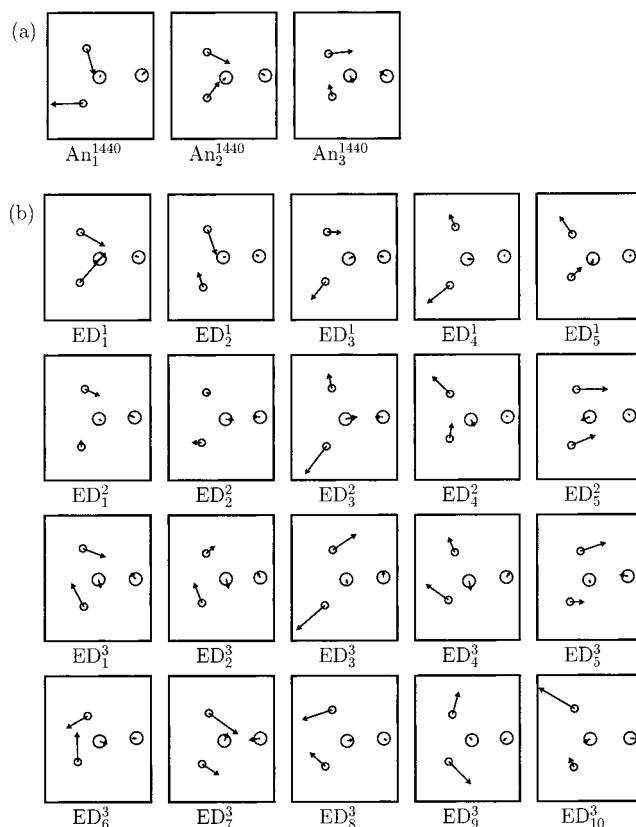
(66) Petersson, G. A.; Tensfeldt, T. G.; Montgomery, J. A., Jr. *J. Am. Chem. Soc.* **1992**, *114*, 6133.

Figure 2. Initial positions and velocities of the carbon (large circles) and deuterium (small circles) atoms in (a) the three vinylidene anion free dynamics trajectories (An_{1-3}^{1440}) and (b) all 20 neutral vinylidene trajectories derived from electron detachment. All atoms lie in a plane.

range. Thus, a maximum 1.0 ps neutral vinylidene trajectory length should provide ample time to observe the dynamics relevant for comparison to experiments using NIPES time scales and somewhat beyond. The total energy was conserved during the entire length of each trajectory (*An* trajectory up to electron detachment plus 1.0 ps from *ED* trajectory) to within 0.1−0.2 kcal/mol (average 0.1 kcal/mol) for the 600 K set and to within 0.1−0.5 kcal/mol (average 0.2 kcal/mol) for the 1440 K set.

During each anion trajectory and the portion of the electron detachment trajectories where the molecule is in the vinylidene well up to the transition state (including re-formed vinylidene, vide infra), we monitored the instantaneous kinetic temperature, T_k, as well as the time-averaged temperature and kinetic energy. In general, the molecule "cooled" slightly after thermal equilibration ceased (more than what could be ascribed to small numerical errors in integrating Newton's equations). This is a consequence of, on average, the molecules sampling higher potential energy regions closer to the barrier, for example. For the electron detachment trajectories initially thermalized at 600 K (3.0 kcal/mol initial kinetic energy), the average kinetic energy was ~2 kcal/mol below the barrier (E_a = 5.6 kcal/mol), with a range of 3.9 kcal/mol below to 0.2 kcal/mol above the barrier top. Not one of these 20 trajectories of 1 ps in length isomerizes! By contrast, when the anion was thermalized at the higher temperature of 1440 K (7.1 kcal/mol), the resulting electron detachment trajectories have average kinetic energies ~3 kcal/mol above the barrier top, with a range of 1.4 kcal/mol below to 7.0 kcal/mol above the barrier top. Despite this excess kinetic energy, only four of the 20 trajectories isomerize! The low probability of isomerization observed here confirms recent quantum dynamics studies[19] which also−coincidentially−yield
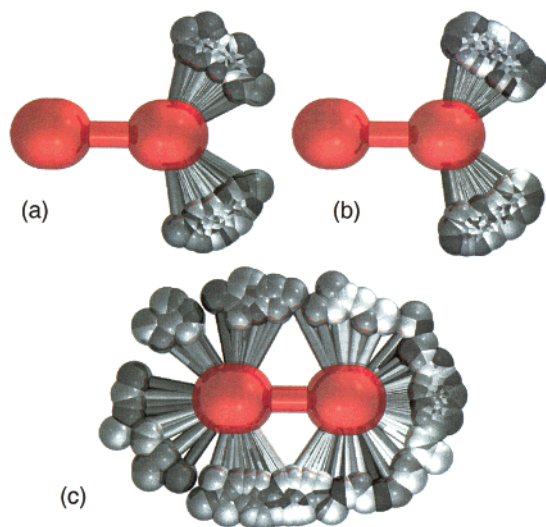
Figure 3. (a) Vinylidene anion trajectory (An_{1-3}^{1440}), (b) nonisomerizing neutral vinylidene trajectory (ED_4^2), and (c) isomerizing neutral vinylidene trajectory (ED_3^3). Each image superimposes the position of the carbon (red) and deuterium (dark to light gray in time) at 10 fs intervals, referenced for visual clarity to a fixed direction and midpoint of the CC bond. *The large amplitude motions of the D atoms in trajectory (c) are clearly seen—a signature of isomerization and barrier recrossing.*

a 20% probability of fast isomerization. The majority of our subsequent analysis focuses on those trajectories initially thermalized to 1440 K, since they exhibit the more interesting isomerization behavior.

Trajectories Starting from the Neutral Transition State. Generally, the photodetachment of the electron from $D_2C=C^-$ will create a vibrationally excited neutral vinylidene that is not at the isomerization TS. For comparison, 10 trajectories starting from the CASSCF(10/10) isomerization transition state, with the same initial velocities as 10 of the electron detachment trajectories generated at 1440 K (with the total angular and linear momentum set to zero), were followed for 220 fs backward and 220 fs forward in time. The initial velocities were carefully chosen to demonstrate distinct types of molecular motion. On average, the kinetic energy for the portion of each transition state trajectory in the vinylidene well (up to the TS) is 6.2 kcal/mol, with a range 3.4−9.4 kcal/mol. Each run will be referred to as $TS^{ed_v^n}$ where ed_v^n refers to the corresponding electron detachment trajectory from which the initial velocities were taken.

Representative Trajectories. Figure 3 graphically displays the results of three representative trajectories, An_3^{1440}, ED_4^2, and ED_3^3 by superimposing the atoms at 10 fs intervals during the simulation, where again An_3^{1440} is the free dynamics part of an anion trajectory, and the ED trajectories follow the evolution of neutral vinylidene after electron detachment. (To obtain a better feel of the complicated dynamics, a movie of ED_3^3 is also available on the web at http://www.chem.ucla.edu/carter/movies.html.) While ED_4^2 certainly is energized, only ED_3^3 (of the trajectories in Figure 3) isomerizes and crosses the barrier multiple times (discussed below). We used these three trajectories to construct anharmonic vibrational frequencies, to see if the vibrational spectra correlate with the very different sets of motion displayed in Figure 3.

E. Vibrational Spectra of Vinylidene Anion and Vinylidene. As described in Section II, we constructed vibrational spectra from the trajectories of Figure 3: a free dynamics
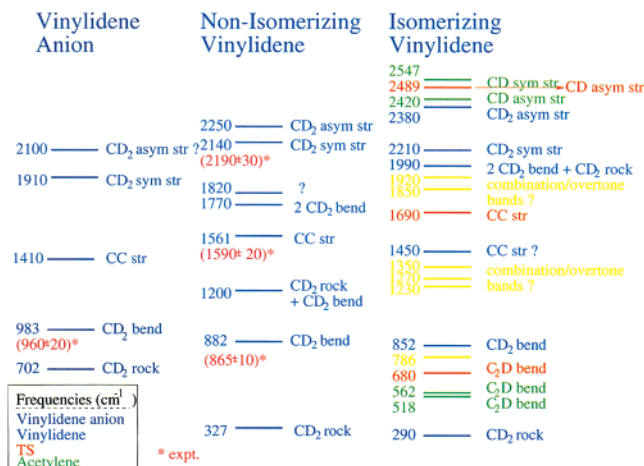

Figure 4. Summary of the anharmonic frequencies and possible assignments extracted via the AIMD-FD technique for vinylidene anion (An_3^{1440}, Figure 5), nonisomerizing vinylidene (ED_4^2, Figure 6), and isomerizing vinylidene (ED_3^3, Figure 7). Frequencies colored according to origin: blue (vinylidene or vinylidene anion), orange (TS), green (acetylene), and yellow (possibly overtone and combination bands). *Notice the increasing spectral congestion going from the anion across to the isomerizing vinylidene.*
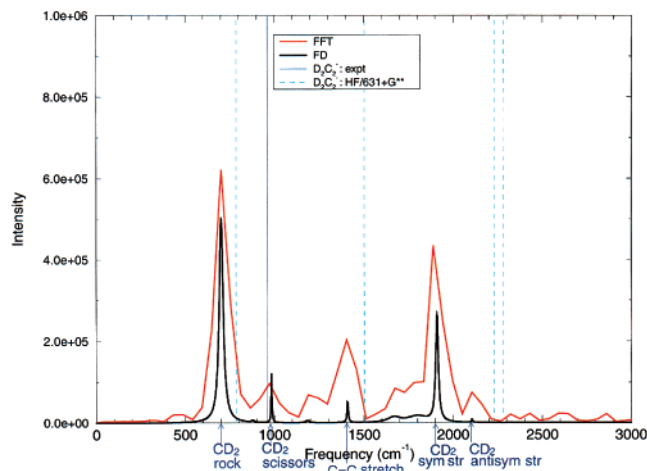

Figure 5. FFT (red) and FD (black) vibrational spectra compared to harmonic normal mode (ref 8, light blue dashed lines) and experimental (ref 8, dark blue solid line) frequencies for $D_2C=C^-$ (from An_3^{1440}). Frequencies of $D_2C=C^-$ extracted via the FD technique are marked with blue arrows corresponding to the color scheme of Figure 4. *Note the large shifts due to anharmonicity and the good agreement with experiment for the CD_2 scissors mode.*

vinylidene anion trajectory (An_3^{1440}; 543 points ≈ 657 fs), a nonisomerizing vinylidene trajectory (ED_4^2; 827 points ≈ 1 ps), and an isomerizing vinylidene trajectory (ED_3^3; 827 points ≈ 1 ps). Figure 4 summarizes the fully anharmonic frequencies extracted via the FD technique. Note the increasing spectral complexity going from the vinylidene anion to the nonisomerizing to the isomerizing vinylidene. Successful isomerization dynamics leads to a congested spectrum, including the appearance of new peaks due to the TS and the product, as well as the disappearance/reduction of some reactant peaks. Figures 5−7 show the FFT and FD spectra for the $D_2C=C^-$ trajectory (An_3^{1440}), the energized yet nonisomerizing $D_2C=C$: trajectory (ED_4^2), and the isomerizing $D_2C=C$: trajectory (ED_3^3), respectively. In each case, the FD gives a more refined spectrum that

New View of the H₂C=C: → HC≡CH Rearrangement

J. Am. Chem. Soc., Vol. 123, No. 4, 2001 **651**

Non-Isomerizing, Neutral Vinylidene Vibrational Spectra

Figure 6. FFT (red) and FD (black) vibrational spectra compared to CASSCF(10/10) harmonic normal mode (this work) and experimental (ref 8) frequencies (vertical lines) for nonisomerizing $D_2C=C$: (ED_4^2). Frequencies of $D_2C=C$: extracted via the FD technique are marked with blue arrows corresponding to the color scheme of Figure 4. *Isomerization is easily ruled out, since peaks corresponding to acetylene vibrations (green dashed lines) do not appear.*

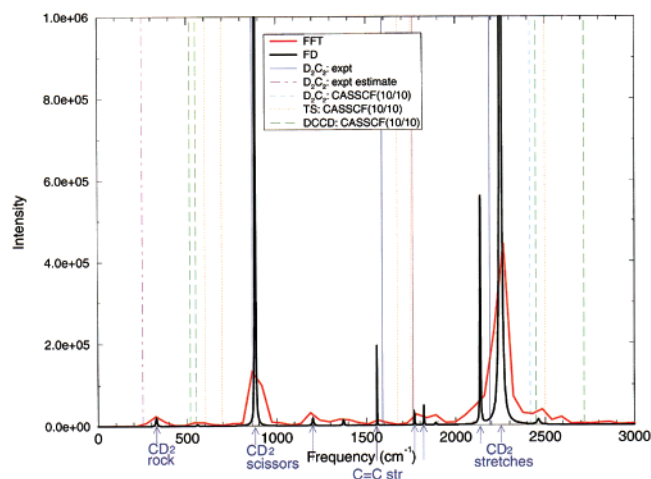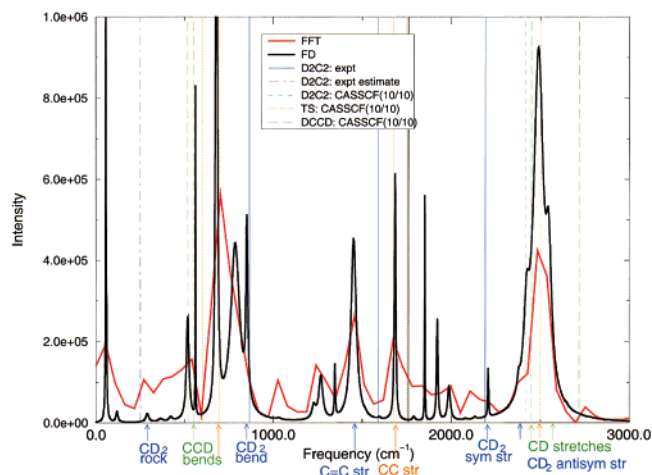Isomerizing, Neutral Vinylidene Vibrational Spectra

Figure 7. FFT (red) and FD (black) vibrational spectra compared to CASSCF(10/10) harmonic normal mode (this work) and experimental (ref 8) frequencies (vertical lines) for isomerizing $D_2C=C$: (ED_3^3). Frequencies of $D_2C=C$: extracted via the FD technique are marked with colored arrows corresponding to Figure 4 according to probable assignment: vinylidene (blue), TS (orange), and acetylene (green). *Note the appearance of bands corresponding to DCCD, D₂CC, and the TS, indicating extensive barrier recrossing.*

is consistent with the FFT results. The frequencies reported in Figure 4 should be viewed as estimates, since they are derived from the analysis of a single trajectory for each species. The ν_4 wag frequencies are not extracted since all the molecules were constrained to be planar in our simulation (since the reaction coordinate is two-dimensional). Although the spectral intensities are not directly comparable to experimental results, the intensities do hint at vibrational modes that potentially dominate the dynamics.

Spectra of vinylidene anion (from An_3^{1440}) are shown in Figure 5. The vinylidene anion spectrum is extremely simple, consisting of the CD₂ rock at 702 cm⁻¹ (ν_6), the CD₂ scissors at 983 cm⁻¹ (ν_3), the CC stretch at 1410 cm⁻¹ (ν_2), the CD₂

symmetric stretch at 1910 cm⁻¹ (ν_1), and possibly the CD₂ asymmetric stretch at 2100 cm⁻¹ (ν_5)[67]. As expected, the anharmonic frequencies are lower than the HF harmonic frequencies, which typically overestimate frequencies by ~10%. The only available experimental frequency (960 ± 20 cm⁻¹)[8] is for the CD₂ scissors mode, which is in good agreement with our calculated frequency of 983 cm⁻¹. The presence of the in-plane π electron (see Figure 1) results in the CD₂ rock being considerably stiffer in the anion than in the neutral vinylidene (compare in Figure 4: 702 vs 327 cm⁻¹). Note that the peaks corresponding to the CD₂ rock (702 cm⁻¹) and CD₂ scissors (983 cm⁻¹) are significantly more pronounced than the CC stretch (1410 cm⁻¹). According to Carrington et al.,[17] exciting the CD₂ rock and CD₂ scissors modes should decrease vinylidene's lifetime, while exciting the C=C stretching mode should increase its lifetime. These trends are easily understood, since both the CD₂ rock and scissors modes are closely related to the isomerization coordinate, thereby facilitating isomerization, while exciting the C=C stretch on average elongates the C−C bond, thereby distorting it away from either an acetylenic or TS-like structure, resulting in an increased lifetime of vinylidene. We shall come back to this issue later on.

The nonisomerizing vinylidene spectra (ED_4^2) in Figure 6 provide further insight into the dynamics of the isomerization. Just like the anion, the CD₂ scissors (882 cm⁻¹) agrees well with experiment (865 ± 10 cm⁻¹)[8]. Removal of the in-plane π electron eliminates the electron−electron repulsion between the C−D bond and the π electron. This is readily apparent in both the dramatically red-shifted CD₂ rock frequency (327 cm⁻¹ vs 702 cm⁻¹) and the red-shifted CD₂ scissors (882 cm⁻¹ vs 983 cm⁻¹) relative to the anion. Likewise, the C=C stretch is blue-shifted by ~150 cm⁻¹ from the anion since the bond shortens when the π electron is removed. Vibrational excitation is revealed further by the appearance of several combination and overtone bands. The explanation about why this neutral vinylidene trajectory (ED_4^2) did not isomerize within 1 ps might lie in the smaller intensity of the favorable CD₂ rock (327 cm⁻¹) compared to the less advantageous CD₂ scissors (882 cm⁻¹) and the inhibiting C=C stretch (1561 cm⁻¹) modes.

Spectra derived from a trajectory where vinylidene isomerizes (ED_3^3) are shown in Figure 7. They are starkly different than spectra derived from a nonisomerizing trajectory. Most importantly, the spectra are far more congested, with the appearance of DC≡CD, D₂C=C:, and TS modes. Vibrational excitation of the neutral vinylidene is apparent in the appearance of combination and overtone bands. The small, but visible CD₂ rock intensity arises from recurrence of the vinylidene structure, as discussed below. In addition, the C−C−D bends in acetylene enhance the recrossing of the transition state (vide infra).[15] Finally, the significant blue-shifting (>100 cm⁻¹) and broadening of the C−C stretch relative to the nonisomerizing vinylidene's C−C stretch is explained by the shortening of the vinylidene C−C double bond as it gains acetylene triple bond character.

Although our anharmonic vibrational frequencies in Figure 4 are not directly comparable to the fine structure of Schork and Köppel's[19] quantum-wave packet-derived photoelectron spectrum, since they studied hydrogenated, not deuterated vinylidene, several interesting comparisons can be made. Our anharmonic frequencies for the CC stretch and the CD₂/CH₂ scissors modes agree slightly better with experiment than Schork

---

(67) The small intensity and additional uncertainty in frequency (2090−2120 cm⁻¹) arises from shifting frequencies in the overlapping energy bins during the FD analysis.

Table 4. Percentage of Time Each Vinylidene Vibrational Normal Mode Is Dominant in the Vinylidene Region of the Trajectories (Mode Dominance Determined via the Scalar Product Method (M_D) Described in Section II)

trajectories		CD_2 rock	CD_2 scissors	CC bond	CD symmetric stretch	average kinetic energy (kcal/mol)
		600 K				
neutral non-isomerizing trajectories	average	18.1	39.1	18.4	9.1	3.7
	range[a]	1.1−59.5	0.6−82.6	1.0−58.6	3.4−18.1	1.7−5.8
		1440 K				
neutral non-isomerizing trajectories[b]	average	4.0	38.3	20.8	12.3	8.2
	range	0.4−23.7	0.1−78.5	0.6−54.1	3.5−21.6	4.2−12.6
		1440 K				
neutral isomerizing trajectories[c]	average	37.1	24.5	10.1	7.8	8.5
ED_1^3		50.1	20.6	9.7	4.6	8.5
ED_2^3		29.4	23.1	15.0	7.5	6.3
ED_3^3		37.6	17.6	16.4	9.7	10.8
ED_4^3		28.5	31.3	5.8	9.8	7.6
		1440 K				
transition-state trajectories[d]	average	39.5	22.6	11.9	10.5	6.2
	range	17.9−94.9	4.8−34.3	0.0−15.9	0.0−22.2	3.4−9.4

[a] Minimum and maximum percentage of time dominant in the non-isomerizing trajectories; e.g. one of the trajectories had the CD_2 rock dominant during only 1.1% of the trajectory, while one had this mode dominant 59.5% of the trajectory. [b] Average from the 16 non-isomerizing neutral electron detachment trajectories. Structure is in the vinylidene region during the entire trajectory. [c] Average from the 4 isomerizing trajectories (ED_1^3−ED_4^3). Vinylidene region defined as the most conservative time interval between the TS ranges listed in Table 5 (32% of the total time). For example, in ED_3^3, the times in the vinylidene region are: 0−37, 420−469, and 887−1000 fs (from Table 5). [d] Average from the 10 transition-state trajectories ($TS^{ed|}$ − $TS^{ed_{10}^3}$). Vinylidene region defined as the time interval between the estimated TS crossings from the vinylidene well listed in Table 6 (42% of total time).

and Köppel's, though their CH_2 rock agrees better with experiment than ours. Their CC stretch (1671 cm⁻¹ in H_2CC:) overshoots experiment (1635 ± 10 cm⁻¹) by 36 cm⁻¹ while ours (1561 cm⁻¹ in D_2CC:) is lower than experiment (1590 ± 20 cm⁻¹) by 31 cm⁻¹. Likewise, our CD_2 scissors (882 cm⁻¹ in D_2CC:) is higher than experiment (865 ± 10 cm⁻¹) by only 17 cm⁻¹, while theirs (1205 cm⁻¹ in H_2CC:) is higher than experiment (1165 ± 10 cm⁻¹) by 40 cm⁻¹. This larger discrepancy for the quantum dynamics simulation might be caused by insufficient sampling of the CH stretch regions of the PES.

Ervin et al. observed a NIPES peak at 370 ± 30 cm⁻¹ that they assigned to the 2 ← 0 transition of the CD_2 rock mode, since the 1 ← 0 fundamental transition is symmetry forbidden. Yet, they could not completely exclude the possibility of symmetry-breaking such that the fundamental transition might be accessed. However, Stanton and Gauss recently showed via extended basis set coupled cluster calculations of an anharmonic ab initio force field that the 2 ← 0 transition is likely to be the correct assignment, assuming temperature effects are unimportant.[58] There is a nontrivial amount of anharmonicity associated with this mode, and hence the 2 ← 0 transition energy is far from twice the 1 ← 0 energy. Schork and Köppel[19] extracted a CH_2 rock frequency (472 cm⁻¹) consistent with the experimentally assigned 2 ← 0 CH_2 rock frequency (450 ± 30 cm⁻¹). Their wave function analysis[18] indicates that the CH_2 rock mode involves 2 or 4 quanta. The lowest frequency in our spectrum of vinylidene (327 cm⁻¹; see Figure 4 and Figure 6) is somewhat lower than the experimental measurement of 370 ± 30 cm⁻¹, but still is suggestive that our AIMD trajectories are also sampling two quanta of CD_2 rock.

In general, though, we find good to excellent agreement with the limited experimental frequencies available. Also, our frequencies provide the best theoretical estimates of the anharmonic frequencies for DC≡CD, D_2C=C:, and D_2C=C⁻ to date.

F. Dynamics Mechanisms. CD_2 Rock Activation. Analysis of the AIMD trajectories, both those formed via anion electron

detachment and those started at the actual isomerization transition state, lead to a set of interesting observations about the isomerization mechanism. Figure 2b shows the starting configurations for all 20 neutral vinylidene trajectories initiated via electron detachment from the 1440 K anion trajectories. On the basis of previous studies,[8,13,17,18,66] we expect those trajectories where the CD_2 rock is activated to isomerize most rapidly. As can be seen visually in Figure 2b, the trajectories ED_1^2, ED_{1-2}^3, and ED_4^3 look likely to be reactive, as they exhibit velocities somewhat akin to those in the CD_2 rock.

A more quantitative estimate of which neutral vinylidene modes are activated after electron detachment is provided by $M_D(t)$, defined in section II, as the dominant normal mode at each time t. Table 4, for the 40 electron detachment trajectories, summarizes the percentage of time each normal mode is dominant during the times the molecule is in the vinylidene well. Two important factors, available kinetic energy and activated modes, dictate which trajectories will isomerize. Not one of the electron detachment trajectories initially thermalized to 600 K isomerizes, even though the CD_2 rock is the dominant mode (up to 59.5% of the time) during 5 of the 20 trajectories. The failure to isomerize is due to insufficient instantaneous kinetic energy in the reaction coordinate. The two trajectories that did have average kinetic energy above the barrier (5.8 vs 5.6 kcal/mol) had the CD_2 scissors, not the CD_2 rock, as the dominant mode.

In those trajectories initially thermalized at 1440 K, we might expect the majority to isomerize since the average kinetic energy is significantly above the barrier (~3 kcal/mol). The contrast between mode dominance in the trajectories initially equilibrated at 1440 K that did, versus did not, isomerize, is striking. In those that did not isomerize, the CD_2 rock does not dominate, while the CD_2 scissors does. By comparison, those that do isomerize have the CD_2 rock as the dominant mode, even though the average kinetic energy is nearly identical (8.5 vs 8.2 kcal/mol) to the nonisomerizing trajectories. In all 1440 K trajec-

Table 5. Times (fs) along Reactive Electron Detachment Trajectories at which Vinylidene, the TS, and Acetylene Are Formed[a]

	ED_1^3	no. oscillations/range[b]	ED_2^3	no. oscillations/range	ED_3^3	no. oscillations/range	ED_4^3	no. oscillations/range	av time[c]
D₂CC:		1		2		1		4	0
[D₂CC]‡	30	29−39	134	112−135	61	37−99	291	264−295	129
DCCD	59	1	161	1	127	6	322	1	167
[D₂CC]‡	87	77−96	182	180−184	391	383−420	347	340−350	252
D₂CC:	122	1	208	1	444	1	377	1	288
[D₂CC]‡	155	150−165	233	232−236	486	469−494	412	408−418	322
DCCD	184	1	261	1	526	5	440	2	353
[D₂CC]‡	229	215−266	295	285−302	760	750−887	512	508−515	449
D₂CC:	298	1	318	1	935		532	1	521
[D₂CC]‡	347	334−352	353	336−364			554	549−556	418
DCCD	376	1	392	14			571	1	446
[D₂CC]‡	411	399−417					595	591−617	503
D₂CC:	439	1					634	1	537
[D₂CC]‡	466	460−468					688	662−697	577
DCCD	487	1					714	2[d]	601
[D₂CC]‡	515	513−530					847	842−853	681
D₂CC:	554	1					871	1	713
[D₂CC]‡	580	576−584					896	891−900	738
DCCD	604	2					920	1	762
[D₂CC]‡	676	674−679					953	940−957	815
D₂CC:	706	1					978	1	842
[D₂CC]‡	740	725−746						997−?	740
DCCD	766	1							766
[D₂CC]‡	804	797−838							804
D₂CC:	860	2							860
[D₂CC]‡	989	972−?							989
no.TS crossed	13		5		4		10		
% time CD₂ rock dominant	50.1		29.4		37.6		28.5		

[a] Columns ED_1^3−ED_4^3 contain estimates, based on visual inspection and similarity to the optimized geometries, of when each type of structure was passed. Also shown are the number of times the TS was crossed (no. TS crossed) and the percentage of time the CD₂ rock mode dominated while in the vinylidene well. [b] "no. oscillations/range" refers to two separate cases. If the entry corresponds to a [D₂CC] row, then the range of numbers listed is a rough estimate of when the molecule was in the TS region. Ranges less than ∼15 fs correspond to a crossing with little or no chatter. However, if the entry is in the D₂CC: or DCCD row, it refers to the number of times the molecule passed through the given structure before crossing over the isomerization barrier. [c] Average time to reach the ith recurrence of a given structure. Only those trajectories that passed the recurrence of the structure within 1 ps are included in the average. [d] In ED_4^3 (714 fs), the molecule went to a structure that looked like the TS (732−799), chattered around the TS, and returned to DCCD instead of continuing to recross to D₂CC: as expected.

tories, we find that if the CD₂ rock is not strongly activated (dominant > 25% of the time), isomerization does not occur (at least on the 1 ps time scale). Even though the average kinetic energy is significantly above the barrier top, 80% of the trajectories did not isomerize within the first ps, strongly suggesting that vinylidene's lifetime is generally longer than one ps.

Likewise, nearly all the trajectories started at the TS have a strongly activated CD₂ rock mode in the vinylidene well (see Table 6), which leads to rapid isomerization. Somewhat surprisingly, the average kinetic energy (6.2 kcal/mol) of these TS trajectories lies between the average kinetic energies of the 600 K (3.7 kcal/mol) and 1440 K (∼8.2 kcal/mol) electron detachment trajectories. When we started the TS trajectories at the TS geometry, we automatically populated the modes along the reaction coordinate, thus allowing the vinylidene to isomerize at a lower kinetic temperature on average. In the electron detachment trajectories, the higher kinetic energy allows more of the potential energy surface to be sampled, but often in regions that do not lead to isomerization.

By comparing the persistence of the other vibrational modes in the isomerizing and nonisomerizing trajectories, it is tempting to make the generalizations that (i) the CD₂ scissors and the CC stretch are slightly less activated in those trajectories that isomerize, in partial agreement with the predictions of Carrington et al.,[17] and (ii) the CD stretches do not affect which trajectories isomerize, in opposition to the conjectures of Keifer et al.[16] Care must be taken in the interpretation of the dominant

modes since the vinylidene normal mode classification does not account for anharmonicity and the sample size is relatively small.

Once the CD₂ rock is activated, conventional wisdom has it that the time scale for isomerization should be on the order of one vibrational period, or ∼100 fs. A "road map" containing the time each configuration (vinylidene, the TS, and acetylene) is reached during the four isomerizing trajectories is contained in Table 5. Figure 8b provides a more visual representation of the trajectories based on the position of the deuteria, as a function of time. Taking the z-axis parallel to the CC bond axis, we first define $D_{i,z}$ (see Fig. 8a as the z-coordinate of deuterium (D_a or D_b) relative to the z-coordinate of the bridging deuterium in the TS. Then, a simple classification of the molecular configuration can be inferred from the product $D_{a,z} * D_{b,z}$. When the product is: >0, both C−D bonds point in the same direction and the species is vinylidene; ∼0, the C−D bonds generally are roughly perpendicular and it is near the TS (dotted line); and <0, the C−D bonds point in opposite directions and it is acetylene. In general, this method yields structural assignments that match the visually observed configurations to within 10 fs. The visual representation immediately reveals the extensive barrier recrossing observed.

Formation of Acetylene. Of the four trajectories that isomerized after electron detachment, the time from initial activation of the CD₂ rock to formation of acetylene ranged from 59 to perhaps 322 fs (see Table 5), where formation of acetylene is defined as the time when the molecule first reached
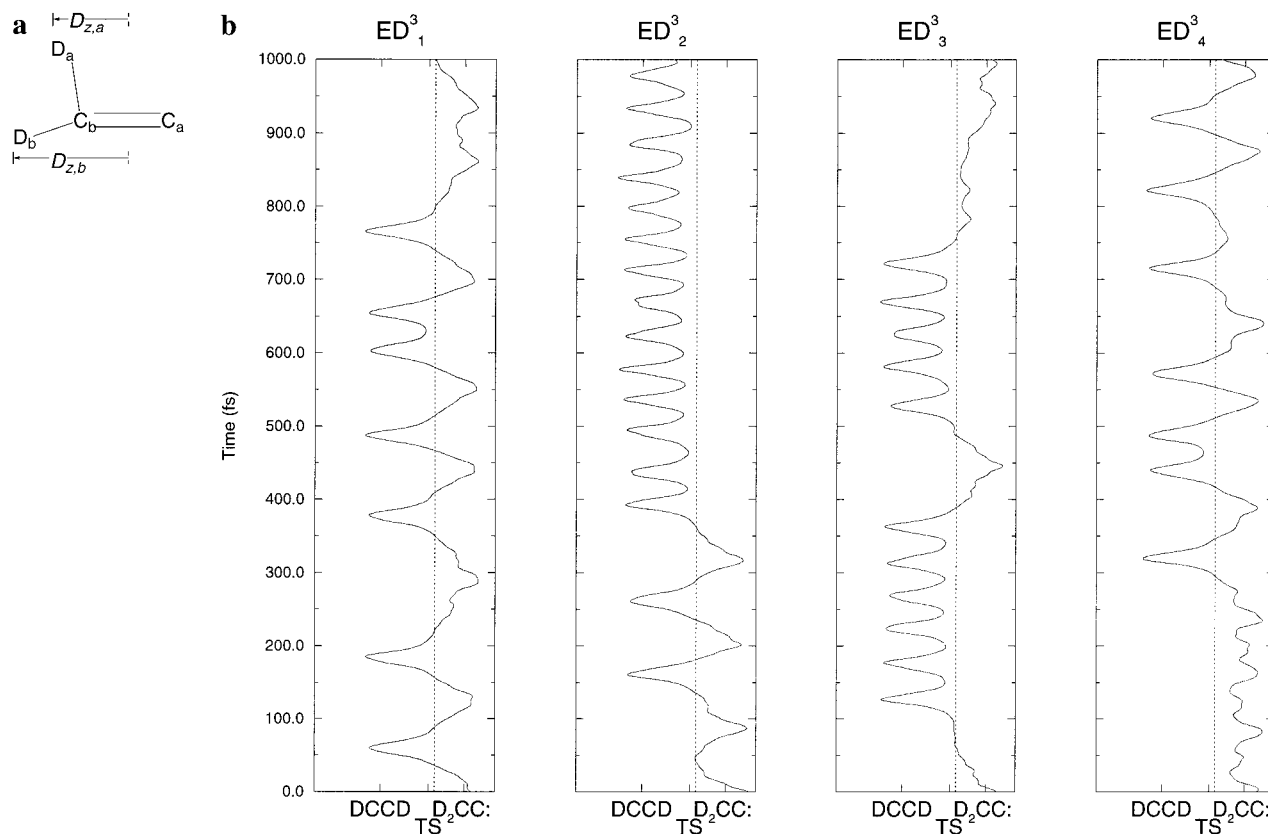
Figure 8. (a) $D_{z,i}$ is the *z*-coordinate of deuterium (D_a or D_b) relative to the *z*-coordinate of the bridging deuterium in the transition state (the TS is 8% displaced from the CC bond midpoint toward C_a), where the *z*-axis is parallel to the CC bond axis. (b) The product, $D_{a,z} * D_{b,z}$, where $D_{z,i}$ is defined in a, is plotted as a function of time for the four 1 ps trajectories that isomerized following electron detachment (ED_1^3, ED_2^3, ED_3^3, ED_4^3). The product, $D_{a,z} * D_{b,z}$, provides a simple means to identify the molecular configuration. For vinylidene, where both deuteria are on the same side of the molecule, $D_{a,z} * D_{b,z} > 0$. For the TS, where one of the deuteria will be in the bridging position, $D_{a,z} * D_{b,z} \approx 0$ (shown by the dotted line). For acetylene, where the deuteria are on opposite sides of the molecule, the z-coordinate of the deuterium vectors will have opposite sign, and hence $D_{a,z} * D_{b,z} < 0$. In general, this method matches the visually observed configurations to within 10 fs. *Note the number of recrossings and significant number of failed isomerization attempts during 1 ps.*

the linear acetylene structure. The short time to formation (ED_1^3) is a case where isomerization occurs how one might expect, namely the CD_2 rocks, goes over the TS, and immediately forms acetylene. However, our simulations show that the dynamics is generally not so simple. One of the trajectories (ED_2^3) nearly reaches the TS, then turns around and then isomerizes on the other side of the C=C bond, resulting in a time to acetylene of 161 fs. Another trajectory (ED_3^3) reaches the TS and then the D atom vibrates around the TS for about 60 fs before going on to acetylene, resulting in a time to acetylene of 127 fs. Indeed, all of these reactive trajectories exhibit some "chattering" of the D atom around the transition-state region, in which the D atom hovers around the TS between $\sim 15-140$ fs before moving on. For example, every crossing of the TS in ED_3^3 exhibited some chattering, where the time spent in the transition-state region is more than 15 fs. Finally, the last reactive trajectory (ED_4^3), has the lowest CD_2 rock dominance (28.5) and the longest initial time to isomerization (291 fs), further indicating the close correlation between the CD_2 rock and the vinylidene lifetime. Later in the trajectory (730−800 fs), the acetylene appears to reach the TS, but reverts back to acetylene, only to recross 50 fs later. Such motion illustrates well the tremendous complexity of the isomerization dynamics.

Neutral TS Trajectories. In the case of the trajectories originating at the neutral TS, the CD_2 rock is almost *always* activated on the vinylidene side of the TS, suggesting again

that CD_2 rock activation is essential to formation of acetylene. Table 6 gives a detailed account of the molecular configuration as a function of time for the TS-originating trajectories. As noted below, all of these trajectories exhibit extensive recrossing of the TS. The one exception to CD_2 rock activation occurs in $TS^{ed_4^3}$, where the molecule stays in the vinylidene well for over 220 fs before crossing the barrier. Once again, this can be explained by the low CD_2 rock mode dominance of only 17.9% and an average kinetic energy for this trajectory of only 5.5 kcal/mol.

Since the CD_2 rock is nearly always activated in these TS cases, we can use the total time spent on the vinylidene side of the TS as an upper bound to the time during which the CD_2 rock is activated. By calculating the time elapsed from the formation of vinylidene to the formation acetylene, using the values in Table 6, we obtain a further estimate of the time to acetylene after activation of the CD_2 rock. In these cases, we find a range of times to reach acetylene of 40 fs to at least 130 fs. Likewise, Schork and Köppel[19] found that activation of the CH_2 rock (2ν) and (4ν) in vinylidene led to lifetimes of 29 and 125 fs respectively, in agreement with our results. Thus, we conclude the CD_2 rock is almost always immediately effective at producing acetylene, and direct isomerization by the shortest path often occurs.

G. Violation of Transition-State Theory. The isomerization dynamics reported here violates completely the conventional notion that once the TS for a highly exothermic reaction is

Table 6. Times (fs) along Backward and Forward Trajectories at which Vinylidene, the TS, and Acetylene Are Formed from the Neutral TS ($t = 0$

	$TS_1^{ed\downarrow}$	$TS_2^{ed\downarrow}$	$TS_4^{ed\downarrow}$	$TS_5^{ed\downarrow}$	$TS_2^{ed\downarrow}$	$TS_2^{ed\uparrow}$	$TS_1^{ed\uparrow}$	$TS_3^{ed\uparrow}$	$TS_4^{ed\uparrow}$	$TS_{10}^{ed\uparrow}$	av time[b]
[D₂CC]‡						220					220
DCCD	179					198					189
[D₂CC]‡	160					182					171
D₂CC:	134					139					137
[D₂CC]‡	91					108					100
DCCD	74	>220	165	152	106	88	71	92		103	106
[D₂CC]‡	52	206	136	111	75	57	47	71		69	92
D₂CC:	19	53	79	54	31	23	17	29	85	29	42
[D₂CC]‡	0	0	0	0	0	0	0	0	0	0	0
DCCD	24	44	54	31	27	22	23	19	47	22	31
[D₂CC]‡	94				120	45		37	63	41	67
D₂CC:	142				160	84		97	133	73	115
[D₂CC]‡	183				>220	117		151	174	99	145
DCCD	203					149		175	202	121	170
[D₂CC]‡						184		197		143	175
D₂CC:						218		>220		169	194
[D₂CC]‡										190	190
DCCD										215	215
no. TS crossed	6	2	2	2	4	8	2	5	3	6	4
% time CD₂ rock dominant	43.7	28.7	36.3	34.8	68.5	48.0	94.9	32.4	17.9	46.2	39.5

[a] Also shown are the number of times the TS was crossed (no. TS crossed) and the percentage of time the CD₂ rock mode dominated while in the vinylidene well. [b] Average time to reach the ith recurrence of a given structure. Only those trajectories that passed the ith recurrence of the structure within 220 fs are included in the average.

traversed, the activated complex is irreversibly converted to products. When one considers energetics only, it is easy to assume that with a small barrier and large exothermicity, the reaction should be irreversible. However, we shall argue that the observed irreversibility depends on the time scale on which the observation is made. We contend that on (sub)picosecond time scales, extensive recrossing of the TS occurs. The recrossing times (defined as the time elapsed between when a "product" has formed and the TS is reached again) in the trajectories derived from electron detachment (Table 5) and from the isomerization TS (Table 6) range from 20 to 600 fs and 16−200 fs, respectively. Thus we find the recrossing usually occurs early and often: in the electron detachment trajectories, all four recross at least once in the first 0.4 ps and recross 3−12 times for trajectories out to 1 ps. In the TS-originating trajectories, each trajectory recrosses a minimum of 1 and a maximum of 7 times, during a period of only 0.44 ps!

The reason for the recrossing in this system can be summarized in a simple picture. After the CD₂ rock induces passage over the barrier and formation of acetylene, the acetylene is highly energized due to the large exothermicity of the reaction. This energy is localized particularly in large amplitude bending motion of the D atom that passed over the TS. This bending motion is so large that the D atom can swing around and recross the TS easily. This is immediately apparent in the movie available at http://www.chem.ucla.edu/carter/movies.html. This picture is entirely consistent with the observations of large amplitude bending motions, with minimal intramolecular vibrational energy redistribution (IVR), in dispersed fluorescence experiments that use lasers to pump energy into acetylene up to near the isomerization barrier.[14,15] Indeed, Holme and Levine[31] also predicted this type of "orbiting motion" of the hydrogens in highly excited acetylene in their classical dynamics simulations. Thus, it is the easy interconversion of the vinylidene CD₂ rock to the large amplitude DCC bending motion in acetylene that leads to the extensive recrossing observed.

Although we often assume microscopic reversibility implies that recrossing the barrier involves following the same exact path, this is absolutely not required. Indeed, generally the TS is reached by pathways that differ somewhat from each other because finite temperature fluctuations make the paths deviate from the Born−Oppenheimer minimum energy path; this further increases the likelihood of recrossing by opening up more reaction channels.

While it is well-known that transition-state theory can fail for reactions in solution,[68] where "solvent friction" can cause extensive recrossing (due to, for example, collisions with solvent molecules), it was not expected to happen here. For gas phase reactions at low pressures, where the thermal energy is comparable to the barrier height (as it is in this case), we claim extensive recrossings are likely to be the rule rather than the exception, unless IVR is very effective at dissipating energy out of the reaction coordinate modes. Thus, transition-state theory should be expected to break down for such cases. This occurs despite the large exothermicity, which would lead one to conclude erroneously that the reaction is irreversible. At higher pressures, or in a "low-friction" liquid solvent, transition-state theory works well because the excess kinetic energy acquired in the formation of product in an exothermic reaction can be dissipated not only by IVR or radiative processes, but also through energy transfer to other molecules via collisions. In the gas-phase simulation we have explored, these other processes are not occurring or are not possible.

H. Reconciliation of Lifetimes. AIMD versus CEI and NIPES. Eventually the vibrational energy in acetylene should redistribute itself into nonproductive modes (e.g., into the CC stretch, etc.) or be lost in fluorescence, as a means of dissipating energy out of the mode associated with the reaction coordinate. When this happens, the reaction may then be termed irreversible. The original NIPES experiment explored the subpicosecond time regime, thus they probably only observed the *first* isomerization of vinylidene to acetylene. However, it appears that the time scale for irreversible conversion to the more stable product, acetylene, is likely to be on the order of microseconds or longer, based on the 3.5 μs lifetime measured by Vager and co-workers

(68) Hynes, J. T. Crossing the Transition State in Solution. In *Solvent Effects and Chemical Reactivity*; Tapia, O., Bertran, J., Eds.; Kluwer: Amsterdam, 1996; pp 231−258.

in their recent CEI experiment.[20] It is highly likely, based on our evidence of extensive recrossing, that what Vager and co-workers measured was simply the result of millions of ultrafast recrossing events by each C_2H_2 species. In this light, it makes complete sense that roughly half of the species would still look like vinylidene, since the particular configuration of the nuclei at the point of collisional ionization would be rather randomly selected from either side of the barrier. Indeed, we find that the four neutral vinylidene trajectories that isomerize and the 10 neutral TS trajectories spend at least ~32% (a conservative estimate) and ~42%, respectively, of their time in a state best described as vinylidene, in moderate agreement with the 51% finding of Vager et al.

Thus, while the initial vinylidene species formed from the C_2H_2 anion may decay quickly to acetylene on the 100 fs time scale, vinylidene is reborn a little while later, over and over again, via the multiple recrossings back from acetylene. Both the NIPES inference of a lifetime on the order of 0.1 ps and the CEI inference of a lifetime beyond 3.5 μs can be made consistent with each other, via a generalized definition of lifetime: the lifetime of vinylidene involves an initial fast decay to acetylene, followed by multiple recrossings back to vinylidene over many orders of magnitude in time, such that vinylidene—not in its "original" state, but vinylidene nonetheless—can exist for much longer than anyone previously suspected. It is clear that one should not interpret the CEI experiments as if vinylidene stays localized in its shallow well for 3.5 μs; on the contrary, the species decays rapidly but just as rapidly recurs, over and over again. Vager and co-workers indeed suggest that recurrences of the vinylidene structure, oscillating between vinylidene and acetylene, may be responsible for their observations.[15,69] Our calculations strongly support that suggestion.

AIMD versus Quantum Wave Packet Dynamics. Our vinylidene lifetime analysis is qualitatively consistent with a number of aspects of Schork and Köppel's quantum dynamics results.[18,19] We see an initial limiting time interval where isomerization does not occur while the atoms are moving to the transition state, the rapid isomerization of those trajectories where the CD_2 rock is strongly energized with sufficient kinetic energy, and the picosecond or longer lifetime of the ~80% remaining vinylidene. However, two limitations of the most recent CCSD(T)-derived PES should be noted: (i) although the PES constructed from CCSD(T) was smooth, a second (albeit) shallow minimum was found along the reaction path, which Schork and Köppel believe is an artifact; and (ii) the PES is truncated with an absorbing potential just beyond the isomerization transition state. The main dynamical consequences of these constraints are that: (i) the artificial extra minimum may affect the predictions, and most importantly, (ii) the dynamics beyond the initial traversal of the transition state, crucial to understanding the measured lifetimes, cannot be considered.

Finally, regarding consequence (i) above, it has been pointed out recently[70] that the single-reference CCSD(T) method should not be used to construct PES's where bonds break and form, as the method becomes unstable for severely stretched bonds. A deeper artificial extra minimum was also found in single-reference MP2 vinylidene-acetylene calculations.[22] This points out the importance of using multireference correlation methods to describe reactions where multiple bonds are broken and formed, as is done in the current work. The use of CASSCF

(69) A similar suggestion is made on page 32 of M. P. Jacobson's Ph.D. Thesis, Massachusetts Institute of Technology, 1999 (http://rwf.lms.mit.edu/group/theses.html).

(70) Dunning, T. H., Jr.; Harding, L. B., during independent lectures at the American Conference on Theoretical Chemistry, June 28, 1999.

ensures a smooth potential surface, which is essential for dynamical studies. While CASSCF molecular dynamics certainly does not provide a panacea of 1 kcal/mol accuracy (errors are more typically a few kcal/mol), the method treats adiabatic, classical systems well (those without hydrogen) and eliminates the problems posed by CCSD(T) potential surfaces.

Second, the quantum dynamics calculations could not address the importance of the barrier recrossing mechanism, since the absorbing potential placed just after the saddle point eliminated the possibility of recrossing. Their model PES is guaranteed to yield an underestimate of the survival probability of vinylidene, since it was assumed that once acetylene was formed, it never reverted to vinylidene. Our work clearly shows this is not a good assumption. On the other hand, in defense of quantum dynamics, tunneling and zero point effects are naturally accounted for.

IV. Concluding Remarks

The rich dynamics we observe for the isomerization of vinylidene to acetylene have both confirmed previous conjectures, such as the importance of the CD_2 rock to isomerization, as well as provide startling, suggestive evidence of the breakdown of transition-state theory due to extensive CD_2 rock—local CCD bend mode coupling. This results in extensive barrier recrossing, which provides the means to reconcile dramatically conflicting estimates of the lifetime of the metastable species vinylidene.

Our simple GVB calculation offers an intuitive origin to the small isomerization barrier: sp^2 to sp rehybridization of the carbenoid lone pair. Similar mechanisms likely play a role in other important rearrangement reactions involving unsaturated molecules (e.g., carbenes, silylenes, and nitrenes). However, this work points out the importance of not just considering the potential energy surface as a means to understand a chemical reaction; examination of the PES alone would have one conclude that such an exothermic reaction must be irreversible. However, because of kinetic energy associated with the vibrational mode coupling, we arrive at completely different conclusions about the nature of this reaction.

Lower bounds on the lifetimes were extracted from NIPES experiments to be ≥0.033 ps and ≥0.027 for D_2C=C: and H_2C=C: respectively, with estimates of subpicosecond lifetimes overall. In our simulations, 100% of the 1 ps trajectories initially thermalized at 600K and 80% of the 1 ps vinylidene trajectories initially equilibrated at 1440 K did not isomerize, despite the average kinetic energy being larger than the barrier for the latter case. Thus, the average lifetime is probably longer than 1 ps, consistent with theoretical[17,18,31] and Ervin et al.'s experimental[8] lower bounds. This makes physical sense, since electron detachment does not prepare vinylidene in a structure close to that of the TS, and hence some time (often >1 ps) is required to redistribute the vibrational energy into the reaction coordinate in order to cross the saddle point. Once this occurs, primarily through excitation of the CD_2 rock, isomerization rapidly follows on the subpicosecond time scale. However, this is not the end of the story. Due to the strong coupling between the CD_2 rock and the acetylene local CCD bend, we find that recrossing occurs multiple times, in violation of conventional transition-state theory.

By contrast to the subpicosecond to picosecond lifetime estimates from the NIPES experiment, the CEI experiment suggested lifetimes for vinylidene at least 6 orders of magnitude longer—living for as long as microseconds. The CEI experiment captured a snapshot 3.5 μs after the birth of vinylidene and saw

that roughly half the molecules were "still" vinylidene. We contend that both the NIPES and CEI measured correct lifetimes—the issue is all in the definition of what is meant by lifetime. The NIPES experiment probes subpicosecond decay of vinylidene, corresponding to the *first time* it traversed the barrier, while the CEI experiment simply captured the thousandth or millionth recurrence of the original vinylidene, suggesting a lifetime >3.5 μs. If one defines the lifetime as how long vinylidene lives before irreversibly becoming acetylene, the latter microsecond lifetime from CEI is relevant, while if one refers to lifetime as the length of time before vinylidene initially converts to acetylene, then the former subpicosecond lifetime from NIPES is appropriate.

A question arises as to whether the observed multiple recrossings are an artifact of the initial high temperature equilibration of the anion. However, this only introduces on average ∼2.7 kcal/mol of excess kinetic energy above the barrier top, not all of which is in the reaction coordinate mode. Once isomerized to acetylene, even those trajectories with kinetic energy just equal to the barrier height suddenly possess >50 kcal/mol kinetic energy. Thus, the additional ∼2.7 kcal/mol represents a small perturbation on the kinetic energy of the newly formed acetylene. We conclude then that the recrossing observed is realistic.

Our predicted anharmonic frequencies for D₂C=C: and D₂C=C⁻ compare favorably with the few available experimental values and offer predictions for the others. The theoretically derived spectra are consistent with the NIPES vibrational fine structure. Moreover, as we also probed dynamics beyond the NIPES time regime, full comparison to experiment will require new measurements that directly probe the picosecond time scale, such as ultrafast vibrational spectroscopy.

The dominant trends in the spectra may be understood as follows. The removal of the in-plane π-electron caused the CD₂ rock to be red-shifted and the C=C stretch to be blue-shifted. During isomerization and recrossing several portions of the potential energy surface were sampled, resulting in the appearance of acetylene, TS, and vinylidene frequencies. We see that AIMD combined with FD can provide spectral signatures to identify reactive events: (i) extra peaks due to the product and/or transition state, (ii) broadening of observed peaks, (iii) and disappearance or significant reduction in size of reactant peaks. When used together, AIMD and FD provide a powerful tool in the interpretation and intuitive understanding of the experimental spectra of ultrafast processes.

To our knowledge, our analysis provides the best estimate of the deuterated vinylidene lifetime to date. More precise results will require prohibitively expensive quantum dynamics on a nine-dimensional, multireference configuration interaction potential energy surface, to account for effects of tunneling, ZPE, out-of-plane motion, vibrational−rotational coupling, and 2.8 kcal/mol overestimation of the barrier height. When such accurate calculations become feasible, the current calculations and associated predictions will provide an important point of comparison. These theoretical lifetimes also await comparison with direct measurements, which, e.g., could be provided by Negative to Neutral to Positive (NeNePo) experiments (also called charge reversal experiments) like those recently conducted on Ag₃.[71] Despite its small size and simple structure, vinylidene exhibits complicated dynamical behavior that continues to challenge our understanding of experiments and conventional theories.

(71) Doo Wan Boo; Ozaki, Y.; Anderson, L. H.; Lineberger, C. *J. Chem. Phys. A*. **1997**, *101*, 6688.

(72) Grev, R. S.; Janssen, C. L.; Schaefer, H. F., III. *J. Chem. Phys.* **1991**, *95*, 5128.